

# A Higher-Order Temporal H-Index for Evolving Networks

Lutz Oettershagen

lutzo@kth.se

KTH Royal Institute of Technology

Stockholm, Sweden

Nils M. Kriege

nils.kriege@univie.ac.at

University of Vienna

Vienna, Austria

Petra Mutzel

petra.mutzel@cs.uni-bonn.de

University of Bonn

Bonn, Germany

## ABSTRACT

The H-index of a node in a static network is the maximum value  $h$  such that at least  $h$  of its neighbors have a degree of at least  $h$ . Recently, a generalized version, the  $n$ -th order H-index, was introduced, allowing to relate degree centrality, H-index, and the  $k$ -core of a node. We extend the  $n$ -th order H-index to temporal networks and define corresponding temporal centrality measures and temporal core decompositions. Our  $n$ -th order temporal H-index respects the reachability in temporal networks leading to node rankings, which reflect the importance of nodes in spreading processes. We derive natural decompositions of temporal networks into subgraphs with strong temporal coherence. We analyze a recursive computation scheme and develop a highly scalable streaming algorithm. Our experimental evaluation demonstrates the efficiency of our algorithms and the conceptual validity of our approach. Specifically, we show that the  $n$ -th order temporal H-index is a strong heuristic for identifying super-spreaders in evolving social networks and detects temporally well-connected components.

## CCS CONCEPTS

• Information systems → Social networks; • Theory of computation → Graph algorithms analysis.

## KEYWORDS

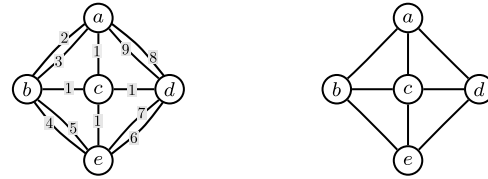
Temporal Network, H-Index, Centrality, Decomposition

## ACM Reference Format:

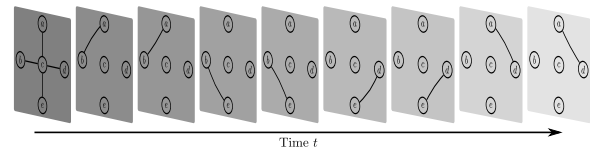
Lutz Oettershagen, Nils M. Kriege, and Petra Mutzel. 2023. A Higher-Order Temporal H-Index for Evolving Networks. In *Proceedings of the 29th ACM SIGKDD Conference on Knowledge Discovery and Data Mining (KDD '23)*, August 6–10, 2023, Long Beach, CA, USA. ACM, New York, NY, USA, 14 pages. <https://doi.org/10.1145/3580305.3599242>

## 1 INTRODUCTION

Measuring the centrality of nodes is one of the fundamental operations in network analysis and has various applications [11, 68]. The H-index was originally proposed by J. E. Hirsch [20] for measuring the productivity and impact of scientists. It is defined as the maximum value  $h$  such that at least  $h$  of the scientist's publications have been cited at least  $h$  times. The corresponding centrality measure for static networks defines the H-index of a node as the maximum value  $h$ , such that at least  $h$  of the node's neighbors have a degree of



(a) A small temporal network. The edges only exist on the indicated time stamps. (b) The underlying aggregated, static graph without temporal restrictions.



(c) The evolving network changes over time. The connectivity under the temporal constraints is restricted and limits the possibilities for the flow of information.

**Figure 1: An example for the  $n$ -th order temporal H-index.** In the temporal network in (a), the 1-st order temporal H-index of node  $c$  is four because  $c$  has four outgoing edges at time one, and each of these edges can be extended by four different edges, each with a strictly later time stamp. Nodes  $a$ ,  $b$ , and  $e$  have a value of two and  $d$  of one. In the aggregate static graph (b), all nodes have a H-index value of three.

at least  $h$ . Recent work has shown that the index yields a successful heuristic for finding super-spreaders in static networks [16, 38, 39]. Recently, Lü et al. [39] formally linked the established concepts of degree centrality, H-index, and the coreness of a node by introducing the  $n$ -th order H-index. The  $n$ -th order H-index is defined recursively using the  $\mathcal{H}$  operator, which, given a multiset  $S$  of integers, returns the maximum integer  $i$  such that at least  $i$  elements in  $S$  are not smaller than  $i$ . So far, the ( $n$ -th order) H-index has been applied primarily to static networks.

However, recently there has been an increasing focus on dynamically changing networks [22, 33, 45]. This trend is motivated by the fact that real-world processes are often inherently dynamic, implying possible causalities that must be taken into account to obtain valid interpretations [22]. Figure 1a shows an example of a small temporal network representing a communication network. The nodes represent persons, and each edge is a bidirectional communication at a specific time shown at the edge. Figure 1c shows the evolution of the network over time. There is a static graph containing the edges with the corresponding time stamp for each time point. Note how temporal evolution restricts the possible flow of information. For example, person  $a$  communicates with  $b$  at time

Permission to make digital or hard copies of part or all of this work for personal or classroom use is granted without fee provided that copies are not made or distributed for profit or commercial advantage and that copies bear this notice and the full citation on the first page. Copyrights for third-party components of this work must be honored. For all other uses, contact the owner/author(s).

KDD '23, August 6–10, 2023, Long Beach, CA, USA

© 2023 Copyright held by the owner/author(s).

ACM ISBN 979-8-4007-0103-0/23/08.

<https://doi.org/10.1145/3580305.3599242>

two and  $b$  with  $c$  at time four, there is a possibility that information flows from  $a$  to  $c$  via  $b$  but not in the reverse direction due to the chronological order of communications—all communications between  $b$  and  $c$  are *after* the communications between  $a$  and  $b$ . If we only consider the underlying aggregated graph, in which the time stamps are removed, and resulting multi-edges are merged (see Figure 1b), there are no restrictions on the possible flow of information. Therefore, in this work, we focus on analyzing *temporal networks* consisting of a set of nodes and a set of temporal edges endowed with time stamps indicating their time of existence. Such temporal networks are prime models of real-world interactions like human contact, communication, and social networks [7–9, 12, 24].

**Current work:** We generalize the  $n$ -th order H-index for temporal networks. First, we introduce the time-dependent in- and outdegrees of a node  $v$  at time  $t$ , counting the number of incoming or outgoing edges before or after  $t$ . On this basis, we define the  $n$ -th order temporal H-index, respecting temporal reachability and possible implied causality. We obtain a family of (1) temporal centrality measures and (2) corresponding core-like temporal decompositions.

The centrality measures based on the  $n$ -th order temporal H-index capture the importance of a node by considering its spatial and temporal position in a neighborhood of depth  $n$  in the network. We propose two variants—the first measures a node’s ability to influence or distribute information, and the second measures how well a node can be influenced or obtain information. The *1-st order temporal H-index* corresponds to the classic static variant with the critical difference that the temporal restrictions in terms of possible incoming or outgoing information flows are respected. For example, in Figure 1a, node  $c$  has four outgoing edges at time  $t = 1$ . Each of the four neighbors also has four outgoing edges at times  $t > 1$ . Hence, any information leaving node  $c$  over one of the four edges at the time one can be further distributed via four edges. Therefore, the 1-st order *outward* temporal H-index is four. With similar arguments, we see that node  $b$ ,  $c$ , and  $e$  have a 1-st order outward temporal H-index of two (e.g.,  $b$  has two outgoing edges to  $e$  at times four and five, and  $e$  has two outgoing edges later than five). Finally, node  $d$  has a value of one. However, suppose we ignore the temporal information and calculate the conventional static H-index in the underlying aggregated static graph shown in Figure 1b. In that case, all nodes obtain the (traditional) H-index value of three, which is uninformative. Furthermore, if we compute the 1-st order *inward* temporal H-index Figure 1a, we obtain a different ranking of the nodes in which  $a$  has the smallest index-value and  $d$  the highest. Note that for the static H-index, there is no such distinction in undirected networks. Going from the 1-st order to higher orders, we can include a deeper neighborhood into the index computation and can identify nodes that have a strong influence in large parts of the network (or can be influenced by large parts of the network in the inward case).

Moreover, a recursive application of the temporal H-index leads to a core-like decomposition of the network. Core decompositions are an essential concept in the study of graph properties with many important applications, e.g., (social) network analysis, community detection, or network visualization [31, 43]. We define the  $(n, k)$ -pseudocore in a temporal network  $\mathcal{G}$  as the maximal induced temporal subgraph such that each node has an  $n$ -th order temporal

H-index of at least  $k$  with respect to  $\mathcal{G}$ . We again propose two variants based on the in- and outward temporal H-index. Our evaluation shows that our  $n$ -th order temporal H-index leads to pseudocores characterized by high temporal reachability.

**Our contributions are:**

- (1) We introduce the  $n$ -th order temporal H-index measuring the importance of nodes based on the structure of their neighborhood respecting temporal reachability. We propose two variants—the first measures a node’s ability to influence or distribute information, and the second measures how well a node can be influenced or obtain information.
- (2) Based on the  $n$ -th order temporal H-index, we introduce a corresponding decomposition of the network into  $(n, k)$ -pseudocores, describing components with high communication capabilities.
- (3) The  $n$ -th order temporal H-index can be straightforwardly computed by directly implementing its recursive formulation. However, this approach is not scalable, and we propose a highly scalable streaming algorithm operating on the chronologically ordered edge stream using only a single pass over the edges.
- (4) Our evaluation on real-world temporal networks shows that our algorithms are highly efficient even for networks with millions of nodes and tens of millions of temporal edges. The  $n$ -th order temporal H-index effectively identifies central nodes and temporally cohesive subgraphs. We demonstrate this in the use case of identifying super-spreaders in epidemic processes in real-world networks.

The omitted proofs are provided in Appendix A.

## 2 RELATED WORK

There are several thorough surveys and introductions to temporal networks, e.g., [22, 33, 45, 67], centrality measures, e.g., [11, 32, 62, 68], and core decompositions [31, 43]. We focus our discussion on techniques for temporal networks closely related to our work.

*Centrality for Temporal Networks.* Several works [29, 50, 70, 71] examine properties of temporal networks, including various temporal centrality measures, and discuss the necessity of considering temporal dynamics. Variants of temporal closeness have been introduced and discussed in [10, 41, 51, 56, 67]. Similar to static closeness, the temporal closeness is often defined as the inverse of the sum of optimal temporal distances. Another path-based centrality measure is betweenness. Buß et al. [6] evaluate the theoretical complexity and practical hardness of computing several variants of temporal betweenness centrality. Santoro and Sarpe [66] discuss the estimation of temporal betweenness. Tsalouchidou et al. [72] extend Brandes’ algorithm [5] for distributed computation of betweenness centrality in temporal networks. Temporal closeness and betweenness only consider *optimal temporal paths*. Our new centralities, in contrast, consider the general temporal reachability of the node itself and its neighborhood, which is more meaningful in settings where information does not necessarily spread along the shortest paths. The Katz centrality [27] measures node importance in terms of the weighted random walks starting (or arriving) at a node. The authors of [4, 19] adapt the walk-based Katz centrality to temporal networks. Rozenshtein and Gionis [65] adapt PageRank for temporal networks by using temporal walks. Oettershagen et al. [54] generalized the random walk betweenness for temporal networks.

These centrality measures are based on *counting temporal walks*, while our  $n$ -th order temporal H-index is based on *counting neighbors with high temporal reachability through  $n$  recursion steps*. Recent works try to identify influential nodes in spreading processes under the influence maximization model for temporal networks [13, 14].

*Temporal Core Decomposition.* Wu et al. [76] proposed  $(k, h)$ -core decompositions for temporal networks, where each node in a  $(k, h)$ -core has at least  $k$  neighbors and at least  $h$  temporal edges to each neighbor. The concept can be interpreted as a weighted static core decomposition and does not take temporal dynamics such as reachability into account. A recent work by Galimberti et al. [15] introduced a notion of temporal span-cores where each core is associated with a time span, i.e., a time interval, for which the coreness property holds. Let  $T$  be the length of the time interval spanned by a temporal graph  $\mathcal{G}$  with edge set  $\mathcal{E}$ , then there is a quadratic number of time intervals for which a temporal span-core can exist, and the asymptotic running times of the proposed algorithms are in  $O(T^2 \cdot |\mathcal{E}|)$  which is prohibitive for large networks. A notable difference to our new approach is that the span-cores decompose a temporal network in its temporal domain such that each vertex may have several distinct span-core values in different time intervals. Whereas our decomposition, similar to the conventional  $k$ -core, leads to a single core number for each vertex.

Core-like concepts are also used in temporal community mining. Hung and Tseng [25] define a temporal community as a  $(l, k)$ -lasting core, which is a  $k$ -core existing for at least  $l$  consecutive time steps and discuss the problem of finding the maximum  $(l, k)$ -lasting core. Qin et al. [61] consider the densest subgraph problem and define a temporal community as an  $(l, \delta)$ -maximal dense core which has an average degree of at least  $\delta$  in a time interval of length at least  $l$ . Qin et al. [60] mine stable communities in temporal networks using the concept of  $(\mu, \tau, \epsilon)$ -stable cores. Here, a node is in a  $(\mu, \tau, \epsilon)$ -stable core if it has no less than  $\mu$  neighbors that have a similarity of at least  $\epsilon$  to the node in at least  $\tau$  snapshots of the temporal network. Li et al. [36] propose as community model the  $(\theta, \tau)$ -persistent  $k$ -core variant. It is defined for a time interval  $I$  such that a  $k$ -core of size  $\tau$  exists in any subinterval of  $I$  with length  $\theta$ . Computing maximum  $(\theta, \tau)$ -persistent  $k$ -cores is NP-hard.

Our  $n$ -th order temporal H-index leads to a *decomposition that has only a single parameter and allows efficient computation* (see Table 2). Core decompositions are valuable tools, e.g., in social network analysis [69], community detection [63], and network visualization [1]. The previously mentioned approaches do not take temporal reachability explicitly into account, whereas *ours supports this naturally via the  $n$ -th order temporal H-index*.

### 3 PRELIMINARIES

We introduce basic definitions and our notation. We refer to the natural numbers without zero by  $\mathbb{N}$ , and define  $\mathbb{N}_0 = \mathbb{N} \cup \{0\}$ . A (static) graph  $G = (V, E)$  consists of a finite set of nodes  $V$  and a finite set  $E \subseteq \{\{u, v\} \subseteq V \mid u \neq v\}$  of undirected edges. A node  $v \in V$  is *incident to*  $e \in E$  if  $v \in e$ . The degree  $\delta(v)$  of a node  $v \in V$  is the number of edges incident to  $v$ .

### 3.1 Temporal Networks

An *undirected temporal network*  $\mathcal{G} = (V, \mathcal{E})$  consists of a finite set of nodes  $V$  and a finite set  $\mathcal{E}$  of undirected *temporal edges*  $e = (\{u, v\}, t, \lambda)$  with  $u$  and  $v$  in  $V$ ,  $u \neq v$ , *availability time* (or *time stamp*)  $t \in \mathbb{N}$  and *transition time* (or *traversal time*)  $\lambda \in \mathbb{N}$ . The availability time specifies when the transition from  $u$  to  $v$  or  $v$  to  $u$  via the edge is possible. In a *directed* temporal network, a temporal edge has the form  $(u, v, t, \lambda)$  and can be traversed from  $u$  to  $v$  only. For convenience, we primarily consider directed temporal networks in the following, which allow to model undirected edges by means of two symmetric directed edges. The transition time of an edge is the time required to traverse the edge, e.g., in a temporal transportation network the time a vehicle needs between two stops, or in a human contact network the time to give information from one person to another person. Notice that it is reasonable and common to assume a strictly positive transition time as information in standard models cannot be transferred instantaneously. The in- and out-degrees of a node  $v$  count the temporal edges arriving or leaving, resp., at  $v$ . We use  $\delta_{\max}^-(\mathcal{G})$  to denote the maximal in-degree and  $\delta_{\max}^+(\mathcal{G})$  for the maximal out-degree of  $\mathcal{G}$ . We write  $\delta_{\max}^-$  or  $\delta_{\max}^+$  for short if  $\mathcal{G}$  is clear from the context.

Given a (directed or undirected) temporal network  $\mathcal{G}$ , removing all time stamps and traversal times, and merging resulting parallel edges, we obtain the (directed or undirected) aggregated graph  $A(\mathcal{G}) = (V, E_s)$  with  $E_s = \{(u, v) \mid (u, v, t, \lambda) \in \mathcal{E}\}$ .

Given a temporal network  $\mathcal{G} = (V, \mathcal{E})$ , it is common to restrict research questions to a given time interval  $I = [a, b]$ , such that only the temporal subgraph  $\mathcal{G}' = (V, \mathcal{E}')$  with  $\mathcal{E}' = \{(u, v, t, \lambda) \in \mathcal{E} \mid t \geq a \text{ and } t + \lambda \leq b\}$  needs to be considered. We do not include restrictive intervals in the following definitions for better readability. However, our definitions and algorithms can be easily adapted to consider only temporal edges starting and arriving within the interval. A *temporal walk* of length  $\ell$  in a temporal network  $\mathcal{G}$  is an alternating sequence  $(v_1, e_1, \dots, e_\ell, v_{\ell+1})$  of nodes and temporal edges connecting consecutive nodes, such that for  $1 \leq i < \ell$ ,  $e_i = (v_i, v_{i+1}, t_i, \lambda_i) \in \mathcal{E}$  and  $e_{i+1} = (v_{i+1}, v_{i+2}, t_{i+1}, \lambda_{i+1}) \in \mathcal{E}$ , and the time constraint  $t_i + \lambda_i \leq t_{i+1}$  holds. Let  $\Delta(\mathcal{G})$  be the *temporal diameter* of  $\mathcal{G}$ , i.e., the length of the longest (in terms of number of edges) temporal walk in  $\mathcal{G}$ .

### 3.2 The H-Index and $k$ -Core Decomposition

A  $k$ -core of a graph  $G$  is a maximal subgraph  $G_k$  of  $G$ , such that every node in  $G_k$  has at least  $k$  neighbors in  $G_k$ . A node  $u$  has *core number*  $c(u) = k$  if  $u$  belongs to a  $k$ -core but not the  $k + 1$ -core of the graph [43]. The core numbers of all nodes can be computed in  $O(|V| + |E|)$  time [3].

Lü et al. [39] showed a relationship between degree centrality, H-index, and core numbers. To this end, they introduced the  $\mathcal{H}$  operator, which essentially represents the calculation of the H-index. Let  $\mathcal{S}$  be the set of finite multisets of integers. The function  $\mathcal{H}: \mathcal{S} \rightarrow \mathbb{N}_0$  returns for a finite multiset of integers  $S \subseteq \{\{s \mid s \in \mathbb{N}_0\}\}$  the maximum integer  $i$  such that there are at least  $i$  elements  $s$  in  $S$  with  $s \geq i$ . We define  $\mathcal{H}(\emptyset) = 0$ .

Using the  $\mathcal{H}$  operator, the H-index of a node  $u$  is defined as  $H(u) = \mathcal{H}(\{\{\delta(v) \mid v \in V \text{ and } v \text{ is neighbor of } u\}\})$ . The  $n$ -th order H-index  $s_u^{(n)}$  of a node  $u$  in a static graph is defined recursively [39].

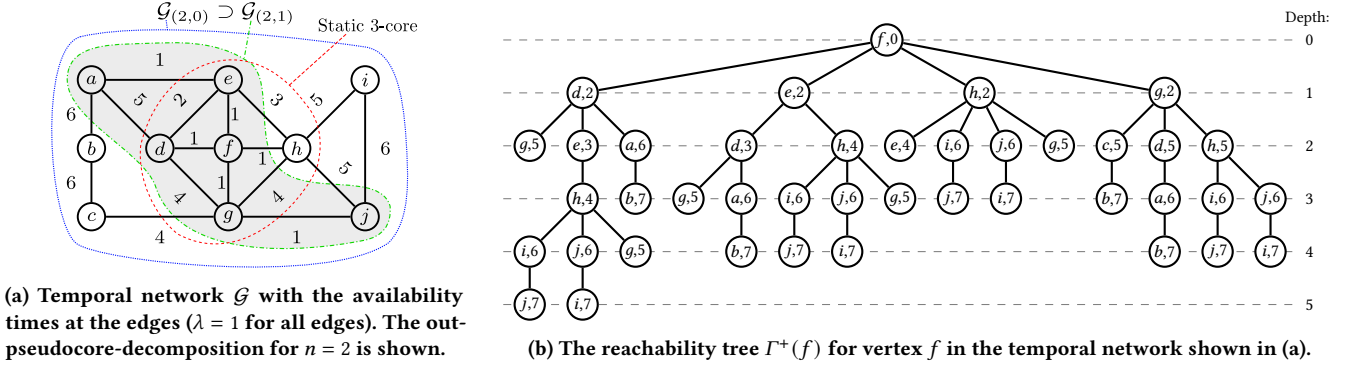


Figure 2: Toy example for the  $n$ -th order temporal H-index. Table 1a shows the corresponding values for all vertices.

Let  $s_v^{(0)} = \delta(v)$  the degree of node  $v$ , then

$$s_u^{(n)} = \mathcal{H} \left( \left\{ s_v^{(n-1)} \mid v \in V \text{ and } v \text{ is neighbor of } u \right\} \right).$$

For  $n = 0$  and  $n = 1$ , the value of  $s_u^{(n)}$  corresponds to the degree and H-index of  $u$ , respectively. For increasing  $n$ , it converges to the *core number* of  $u$  [39].

#### 4 THE $N$ -TH ORDER TEMPORAL H-INDEX

We now define the  $n$ -th order H-index for temporal networks. To this end, we start by generalizing the degree of a node to incorporate the temporal aspects of the local network topology.

**Definition 1.** Given a temporal network  $\mathcal{G} = (V, \mathcal{E})$ , we define the time-dependent in-neighborhood of a node  $u$  at time  $t$  as  $N^-(u, t) = \{(v, u, t_e, \lambda_e) \in \mathcal{E} \mid t_e + \lambda_e \leq t\}$ . Similarly, the time-dependent out-neighborhood is  $N^+(u, t) = \{(u, v, t_e, \lambda_e) \in \mathcal{E} \mid t_e \geq t\}$ . Finally, we define  $\delta^-(u, t) = |N^-(u, t)|$  and  $\delta^+(u, t) = |N^+(u, t)|$  the time-dependent in- and out-degree, respectively.

The time-dependent out-degree of  $u$  reflects the number of ways to extend a temporal walk from  $u$  at or after time  $t$  by an edge. The time-dependent in-degree counts the number of edges via which a temporal walk can reach  $u$  no later than at time  $t$ . Furthermore, we define sets of nodes with time stamps that allow extending walks.

**Definition 2.** We define the multiset  $\mathcal{N}^+(v, t)$  that contains all pairs of nodes and times  $(w, t_w)$  such that there is a temporal edge  $(v, w, t', \lambda) \in \mathcal{E}$  with arrival time  $t_w = t' + \lambda$  and  $t' \geq t$ . Analogously, we define the multiset  $\mathcal{N}^-(v, t)$  that contains all pairs of nodes and starting times  $(w, t_w)$  such that there exists a temporal edge  $(w, v, t_w, \lambda) \in \mathcal{E}$  with  $t_w + \lambda \leq t$ .

Using the Definitions 1 and 2 together with the  $\mathcal{H}$  operator, we define the  $n$ -th order temporal H-index.

**Definition 3.** Let  $(\square, \star) \in \{(0, +), (\infty, -)\}$ . The  $n$ -th order temporal H-index of a node  $v \in V$  is defined as  $h_{v, \star}^{(n)} = h_{v, \square, \star}^{(n)}$  with

$$h_{v, \star}^{(n)} = \mathcal{H} \left( \left\{ h_{w, t_w, \star}^{(n-1)} \mid (w, t_w) \in \mathcal{N}^\star(v, t) \right\} \right).$$

We define  $h_{v, \star}^{(0)} = \delta^\star(v, t)$ .

We call  $h_{v, +}^{(n)}$  the *outward*  $n$ -th order temporal H-index and  $h_{v, -}^{(n)}$  the *inward*  $n$ -th order temporal H-index. Note that also for undirected temporal networks typically  $h_{v, +}^{(n)} \neq h_{v, -}^{(n)}$  due to the direction implied by the temporal information.

The  $n$ -th order temporal H-index equals the (in-/out-) degree centrality in the case of  $n = 0$ . For  $n = 1$ , we obtain time-directed variants of the classical H-index. For larger  $n$ , intuitively, a node  $v$  has a high index value if it is in a temporally well-connected position in the network. More precisely, for the outward variant,  $v$  can reach many other nodes with temporal walks of length  $n + 1$ , and this recursively holds for the reachable nodes (with reduced walk length). Therefore, nodes with high outward temporal H-index can strongly influence their neighborhood, e.g., spread information easily, and are connected to similarly influential nodes. Analogously, a node  $v$  has a high inward index value if the node can be reached by many other nodes with temporal walks of length  $n + 1$ , and this recursively holds for the nodes reaching  $v$  (with reduced walk length). Hence, nodes with high inward temporal H-index can easily obtain information, i.e., be influenced, and are also connected to nodes with a similar ability. For both variants, the influence of temporal walk counts is controlled by the iterated application of the  $\mathcal{H}$  operator based on the temporal structure of the neighborhood. We determine the exact lower bounds of the number of reachable nodes in Theorem 1. Figure 2a gives an example of a temporal network, and Table 1a shows the outward temporal H-index values of the nodes for  $n \leq 4$ .

Table 1b shows the values of the static  $n$ -th order H-index for the underlying static graph  $A(\mathcal{G})$ , ignoring the temporal information. The values of the H-index ( $n = 1$ ) and  $k$ -core numbers ( $n = 2$ ) differ for all nodes. Likewise, for  $n = 1$ , the *rankings* of the nodes disagree, as in the static case, the nodes are only ranked in three groups (i.e., nodes with value 2, 3, or 4) and in the temporal case in four (i.e., nodes with values 0, 1, 2, or 3, respectively). For  $n = 2$ , the decompositions differ in the nodes  $a$ ,  $h$ , and  $j$ . As Figure 2a shows, the most inner core  $\mathcal{G}_{(n,1)}$  (for  $n = 2$ , highlighted in green) contains both  $a$  and  $j$ , but not  $h$ . The static  $k$ -core decomposition decomposes the graph into two groups of nodes with core numbers two and three. The most inner core, i.e., induced by nodes with the core number  $k = 3$ , contains  $h$  but not  $a$  and  $j$  (highlighted in red).

**Table 1: The values of the static and temporal H-index for the example shown in Figure 2.**

(a) The values  $h_{v,+}^{(n)}$  of the outward  $n$ -th order temporal H-index.

$n$	n-th Order Temporal H-index $h_{v,+}^{(n)}$									
	$a$	$b$	$c$	$d$	$e$	$f$	$g$	$h$	$i$	$j$
0 (degree)	3	2	2	4	4	4	5	5	2	3
1	1	0	0	1	2	3	2	1	0	1
2	1	0	0	1	1	1	1	0	0	1
3	1	0	0	1	0	1	0	0	0	1
4	0	0	0	0	0	1	0	0	0	0

(b) The values  $s_v^{(n)}$  of the  $n$ -th order static H-index computed in the underlying static graph.

$n$	n-th Order Static H-index $s_v^{(n)}$									
	$a$	$b$	$c$	$d$	$e$	$f$	$g$	$h$	$i$	$j$
0 (degree)	3	2	2	4	4	4	5	5	2	3
1 (H-index)	2	2	2	3	3	4	3	3	2	2
2 ( $k$ -core)	2	2	2	3	3	3	3	3	2	2

## 4.1 Properties

In the following, we investigate the properties of the  $n$ -th order temporal H-index. To this end, we first define a *reachability tree* that represents all outgoing (or incoming) temporal walks from a node  $v \in V$ . The reachability tree is not a data structure used in our algorithms but a valuable tool for illustrating and discussing the  $n$ -th order temporal H-index. All results in this section hold for the outward and inward variants of the  $n$ -th order temporal H-index.

**Definition 4.** Let  $\star \in \{-, +\}$ ,  $\mathcal{G} = (V, \mathcal{E})$  a temporal network,  $v \in V$ , and  $t \in \mathbb{N}_0$ . The tree  $\Gamma^\star(v, t) = (U, E, r)$  with  $U \subseteq \{(u, t') \mid u \in V, t' \in \mathbb{N}_0\}$  is defined recursively as the tree with root  $r = (v, t)$  and a child  $c_i$  for each  $(w_i, t_i) \in \mathcal{N}^\star(v, t)$ , where  $c_i$  is the root of the tree  $\Gamma^\star(w_i, t_i)$ . For  $\star = +$ , we define  $\Gamma^+(v) = \Gamma^+(v, 0)$ , and for  $\star = -$ ,  $\Gamma^-(v) = \Gamma^-(v, \infty)$ .

Let  $d(u)$  be the depth of  $u \in V(\Gamma^\star(v))$ . The tree  $\Gamma^+(v)$  contains a node  $u = (v, t)$  for each node that we can reach at time  $t$  in a temporal walk starting at node  $v$  using  $d(u)$  consecutive temporal edges. For example, Figure 2b shows  $\Gamma^+(f)$  for the node  $f$  of the temporal network in Figure 2a. Similarly,  $\Gamma^-(v)$  contains a node  $u = (v, t)$  for each node that can reach  $v$  with a temporal walk starting at a time  $t$  using  $d(u)$  consecutive temporal edges.

**Definition 5.** Let  $\star \in \{-, +\}$ ,  $\Gamma^\star(v) = (U, E, r)$ ,  $u \in U$ , and  $C(u) \subseteq U$  be the children of  $u$ . For  $n \in \mathbb{N}_0$ , we define  $\phi_n: U \rightarrow \mathbb{N}_0$  as

$$\phi_n(u) = \begin{cases} \mathcal{H}(\{\phi_n(c) \mid c \in C(u)\}), & \text{if } d(u) < n \\ |C(u)|, & \text{if } d(u) = n \\ 0, & \text{otherwise.} \end{cases} \quad (1)$$

The usefulness of  $\Gamma^\star(v)$  together with  $\phi_n$  is given by the following result.

**Lemma 1.** Let  $\star \in \{-, +\}$ ,  $\mathcal{G} = (V, \mathcal{E})$  be a temporal network,  $v \in V$ ,  $\Gamma^\star(v) = (U, E, r)$  be the reachability tree of  $v$ , and  $n \in \mathbb{N}_0$ . Then,  $\phi_n(u = (w, t)) = h_{w,t,\star}^{(n-d(u))}$  for each  $u \in U$  with  $d(u) \leq n$ .

Using  $\Gamma^\star(v)$ , we can state a lower bound based on  $h_{v,\star}^{(n)}$  of the number of different temporal walks of length at most  $n$  starting from node  $v$ .

**THEOREM 1.** Let  $\star \in \{-, +\}$ ,  $\mathcal{G} = (V, \mathcal{E})$  be a temporal network,  $v \in V$ ,  $n \in \mathbb{N}$ , and  $h_{v,\star}^{(n)} = k$ . Then, there are at least  $(k^{(n+2)} - k)/(k - 1)$  descendants  $u \in U$  of the root  $r$  in  $\Gamma^\star(v)$  with  $d(u) \leq n$ .

Each descendant of  $r$  in  $\Gamma^\star(v)$  corresponds to one temporal walk leaving ( $\star = +$ ) or arriving ( $\star = -$ ) at  $v$  in  $\mathcal{G}$ . Hence, the  $n$ -th order temporal H-index, on the one hand, gives a lower bound of outgoing/incoming temporal walks of  $v$ . On the other hand, for each visited node a similar lower bound holds, i.e., each descendant  $u$  of  $r$  with depth  $d_u$  has at least  $\sum_{i=1}^{n-d_u+1} k^i = \frac{k^{n-d_u+2} - k}{k-1}$  descendants.

In static networks, the static  $n$ -th order H-index of a node  $v \in V$  converges to the  $k$ -core value of the node  $v$  for sufficiently large  $n$  [39]. This does not hold for the  $n$ -th order temporal H-index.

**THEOREM 2.** Let  $\star \in \{-, +\}$ ,  $\mathcal{G} = (V, \mathcal{E})$  and  $v \in V$ . It holds that  $h_{v,\star}^{(n)} = 0$  for all  $n > \Delta(\mathcal{G})$ .

Therefore, neither the outward nor the inward  $n$ -th order temporal H-index converges to the  $k$ -core composition of the network.

## 4.2 Temporal Pseudocore Decomposition

The two variants of the  $n$ -th order temporal H-index provide two natural ways of decomposing the temporal network.

**Definition 6.** Let  $\star \in \{-, +\}$ ,  $\mathcal{G} = (V, \mathcal{E})$  be a temporal network, and  $k, n \in \mathbb{N}$ . The temporal  $(n, k)$ -pseudocore of  $\mathcal{G}$  is a maximal induced temporal subgraph  $\mathcal{G}_{(n,k)}$  of  $\mathcal{G}$  such that for all  $v \in V(\mathcal{G}_{(n,k)})$  the  $n$ -th order temporal H-index  $h_{v,\star}^{(n)} \geq k$  in  $\mathcal{G}$ .

We distinguish *in*- and *out*-pseudocores for  $\star = -$  and  $\star = +$ , resp. The following observations and results hold for both variants. For a node  $v$  in a  $(n, k)$ -pseudocore  $\mathcal{G}_{(n,k)}$ , the inequality  $h_{v,\star}^{(n)} \geq k$  does not hold necessarily with respect to  $\mathcal{G}_{(n,k)}$ . However, each  $(n, k)$ -pseudocore is a subset of nodes that implies a temporal subgraph containing nodes with similar temporal activity and importance in the network  $\mathcal{G}$ . In Section 5.4, we show that the pseudocore can be used to identify temporally well-connected subgraphs.

**Definition 7.** For a fixed  $n \in \mathbb{N}$ , the temporal pseudo-degeneracy  $\tau_n$  of a temporal network  $\mathcal{G}$  is defined as the maximum  $k$  for which  $\mathcal{G}$  contains a non-empty  $(n, k)$ -pseudocore. Similarly, for a fixed  $k \in \mathbb{N}$ , we define the order pseudo-degeneracy  $\eta_k$  as the maximum  $n$  for which  $\mathcal{G}$  contains a non-empty  $(n, k)$ -pseudocore.

We show the following containment properties.

**THEOREM 3.** Let  $\mathcal{G} = (V, \mathcal{E})$  be a temporal graph and  $k, n \in \mathbb{N}$ . For  $n \in \mathbb{N}$  fixed, it holds  $\mathcal{G}_{(n,0)} \supseteq \mathcal{G}_{(n,1)} \supseteq \dots \supseteq \mathcal{G}_{(n,\tau_n-1)} \supseteq \mathcal{G}_{(n,\tau_n)}$ , and for  $k \in \mathbb{N}$  fixed,  $\mathcal{G}_{(0,k)} \supseteq \mathcal{G}_{(1,k)} \supseteq \dots \supseteq \mathcal{G}_{(\eta_k-1,k)} \supseteq \mathcal{G}_{(\eta_k,k)}$ .

Figure 2a shows an example of the out-pseudocore decomposition for  $n = 2$ , and Table 1b shows the core numbers of the (conventional)  $k$ -core decomposition of the underlying aggregated graph  $A(\mathcal{G})$  that ignores the temporal information. Note the differences for nodes  $a, j$ , and  $h$  between the rankings of the static  $k$ -core and the temporal out-pseudocore (note that we compare

**Table 2: Overview of the algorithms for computing the  $n$ -th order temporal H-index and their properties ( $\star = -$  for the inward variant and  $\star = +$  for the outward variant.)**

Algorithm	Running Time	Space	Edge Trans. Times	Results for $\forall i \in [n]$
RECURS	$\mathcal{O}( V n(\delta_{\max}^{\star})^2)$	$\mathcal{O}( V n\delta_{\max}^{\star})$	individual	$\times$
STREAM	$\mathcal{O}( \mathcal{E} n\delta_{\max}^{\star})$	$\mathcal{O}( V n\delta_{\max}^{\star})$	uniform	$\checkmark$

the relative rankings and not the core values, which are not directly comparable) resulting from the conceptual differences of the out-pseudocore and the conventional  $k$ -core.

### 4.3 Computation

We discuss two algorithms with different properties and running times for computing the  $n$ -th order temporal H-index. Both algorithms can be used to compute the inward and outward variants. The first algorithm RECURS is a straightforward implementation of the recursive formulation. We additionally use memoization to avoid redundant computations. However, the running time of RECURS still is unsatisfactory. Therefore, we introduce a highly efficient one-pass streaming algorithm based on the *edge stream representation* of temporal networks, which represents the temporal network as a chronologically ordered list of the temporal edges (ties are broken arbitrarily). The edge stream representation is commonly used for temporal graph streaming algorithms, e.g., [49, 54, 75]. Our streaming algorithm leads to significantly improved running times compared to the recursive algorithm (see Section 5.1). It only supports temporal networks with equal transition times for all temporal edges. However, this is a common property for many real-world temporal networks, e.g., face-to-face contact or email networks.

Table 2 shows an overview of the algorithms and their properties. We provide the pseudocode and a discussion of the running time of RECURS in Appendix B. Both algorithms can be easily adapted to only consider edges in a given interval  $I$ . Alternatively, we can remove all edges not starting or arriving in  $I$  in a preprocessing step in  $\mathcal{O}(|\mathcal{E}|)$  time. Moreover, we assume that no isolated nodes exist, such that  $|V| \leq 2|\mathcal{E}|$ . Because the degree of an isolated node  $v$  is zero, it follows  $h_v^{(i)} = 0$  for all  $0 \leq i \leq n$ . Hence, we can safely remove all isolated nodes in a preprocessing step in  $\mathcal{O}(|V|)$  time.

Table 7 in the appendix gives an overview of the complexities of related temporal centrality measures and core decompositions, showing the competitiveness of our streaming algorithm.

In the following, we assume that  $\lambda = 1$  for all  $e \in \mathcal{E}$ . Algorithm 1 shows the pseudocode of our streaming algorithm. It needs only a single pass over the edges in reverse chronological order, where temporal edges with equal availability times are processed in an arbitrary order. The algorithm computes  $h_{v,+}^{(i)}$  for all  $0 \leq i \leq n$  and  $v \in V$  (note that Algorithm 2 only computes  $h_{v,\star}^{(n)}$  for a fixed  $n$ ). In Appendix B.2, we show how to transform the input to use Algorithm 1 to compute  $h_{v,-}^{(i)}$  for all  $0 \leq i \leq n$  and  $v \in V$ .

A key idea of the algorithm is to keep a single counter for the time-dependent degree for each node. To this end, we use two arrays  $lt$  and  $deg$ ; the former stores the last time  $deg$  was updated, and  $deg$  contains the current time-dependent degree of node  $u$ .

Furthermore, the algorithm manages a list  $\pi[v][i]$  of pairs  $(t', x)$  of  $i$ -th order  $H$ -indices for  $0 \leq i \leq n+1$  and for all  $v \in V$ . Here, the time  $t'$  is stored to exclude values during the computation of the  $\mathcal{H}_t$  operator depending on some time  $t$  (see line 1).

**THEOREM 4.** *Algorithm 1 computes  $h_{v,+}^{(i)}$  for all  $0 \leq i \leq n$  and  $v \in V$  in time  $\mathcal{O}(|\mathcal{E}| \cdot n \cdot \delta_{\max}^{\star})$  with space  $\mathcal{O}(|V| \cdot n \cdot \delta_{\max}^{\star})$ .*

---

#### Algorithm 1: Streaming algorithm STREAM

---

**Input:** Temporal graph  $\mathcal{G} = (V, \mathcal{E})$  as ordered edge stream,  $n \in \mathbb{N}$   
**Output:**  $h_{v,+}^{(i)}$  for all  $0 \leq i \leq n$  and  $v \in V$

//  $\mathcal{H}_t(L)$  computes  $\mathcal{H}(L)$  dependent on time  $t$

- 1 **Function**  $\mathcal{H}_t(L)$ :
- 2    $L_t \leftarrow \{x \mid (t', x) \in L \text{ with } t' > t\}$
- 3   **return**  $\mathcal{H}(L_t)$
- 4 Initialize  $lt[v] = \infty$  and  $deg[v] = 0$  for all  $v \in V$
- 5 Initialize list  $\pi[v][i]$  for each  $v \in V$  and  $0 \leq i \leq n+1$
- 6 **foreach**  $e = (u, v, t) \in \mathcal{E}$  in reverse chronological order **do**
- 7   **if**  $lt[u] > t$  **then**
- 8      $lt[u] \leftarrow t$
- 9      $deg[u] \leftarrow \pi[u][0].length$
- 10   **if**  $lt[v] > t$  **then**
- 11      $lt[v] \leftarrow t$
- 12      $deg[v] \leftarrow \pi[v][0].length$
- 13      $\pi[u][0].append((t, 1))$
- 14     **if**  $n = 0$  **then** continue
- 15      $\pi[u][1].append((e.t, deg[v]))$
- 16     **for**  $1 \leq j \leq n$  **do**  $\pi[u][j+1].append((t, \mathcal{H}_t(\pi[v][j])))$
- 17 Initialize  $h_{v,+}^{(i)} = 0$  for all  $v \in V$  and  $0 \leq i \leq n$
- 18 **for**  $v \in V$  **do**
- 19    $h_{v,+}^{(0)} \leftarrow \pi[v][0].length$
- 20   **for**  $1 \leq i \leq n$  **do**  $h_{v,+}^{(i)} \leftarrow \mathcal{H}_0(\pi[v][i])$
- 21 **return**  $h_{v,+}^{(i)}$  for all  $v \in V$  and  $0 \leq i \leq n$

---

## 5 EXPERIMENTAL EVALUATION

We experimentally evaluate the efficiency of our algorithms and the efficacy of the  $n$ -th order temporal H-index.

**Data Sets:** We use a wide range of real-world temporal network data sets from various online and offline domains for our evaluation. Table 3 shows the properties and statistics of the data sets. All data sets are publicly available.<sup>1234</sup> The transition times of the temporal edges are one for all data sets.

**Algorithms:** We implemented the following algorithms in C++ using the GNU CC Compiler 10.3.0.

- RECURS is the implementation of naive recursive algorithm Algorithm 2 (see Appendix B).
- STREAM is the implementation of Algorithm 1.

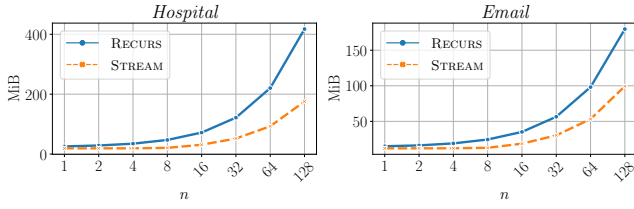
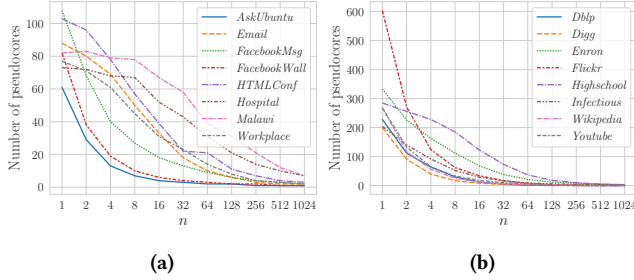
All experiments were performed on a computer cluster. Each experiment had an exclusive node with an Intel(R) Xeon(R) Gold 6130 CPU @ 2.10GHz and 192 GB of RAM. The source code is available at <https://gitlab.com/tgpublic/tgh>.

<sup>1</sup> <https://www.sociopatterns.org>    <sup>2</sup> <https://snap.stanford.edu>

<sup>3</sup> <https://networkrepository.com/dynamic.php>    <sup>4</sup> <http://konect.cc/networks>

**Table 3: Statistics of the data sets** ( $\mathcal{T}(\mathcal{G}) = \{t \mid (u, v, t, \lambda) \in \mathcal{E}\}$ ).

Data set	Properties						Ref.
	$ V(\mathcal{G}) $	$ E(\mathcal{G}) $	$ \mathcal{T}(\mathcal{G}) $	avg. out-deg.	$\delta_{\max}^+(\mathcal{G})$	Domain	
<i>Hospital</i> <sup>1</sup>	75	32 424	9 453	864.6	4 286	face-to-face	[73]
<i>Malawi</i> <sup>1</sup>	84	102 261	43 436	2 434.8	7 932	face-to-face	[55]
<i>Workplace</i> <sup>1</sup>	92	9 827	7 104	213.6	1 091	face-to-face	[17]
<i>HTMLConf</i> <sup>1</sup>	113	20 818	5 246	368.5	1 483	face-to-face	[26]
<i>Highschool</i> <sup>1</sup>	327	188 508	7 375	1 153.0	4 647	face-to-face	[44]
<i>Email</i> <sup>2</sup>	1 866	31 727	18 682	17.0	2 635	communication	[64]
<i>FacebookMsg</i> <sup>3</sup>	1 899	59 798	58 911	31.5	1 091	communication	[57]
<i>Infectious</i> <sup>1</sup>	10 972	415 912	76 944	75.8	616	face-to-face	[26]
<i>FacebookWall</i> <sup>4</sup>	63 731	817 035	333 924	25.6	1 098	messages on user page	[74]
<i>Enron</i> <sup>4</sup>	86 806	1 133 968	213 167	13.1	38 635	communication	[30]
<i>AskUbuntu</i> <sup>2</sup>	134 035	257 305	257 079	1.9	2 358	question answering	[58]
<i>Digg</i> <sup>4</sup>	279 630	1 731 652	6 865	6.2	995	friendship	[21]
<i>Wikipedia</i> <sup>4</sup>	1 870 709	39 953 145	2 198	21.4	6 975	co-editing	[48]
<i>Dblp</i> <sup>4</sup>	1 821 070	11 859 561	49	13.0	2 606	co-authorship	[34]
<i>Flickr</i> <sup>3</sup>	2 302 925	33 140 016	134	14.4	26 367	friendship	[46]
<i>Youtube</i> <sup>3</sup>	3 223 585	9 375 374	203	5.8	91 751	friendship	[47]

**Figure 3: Effect of increasing  $n$  on the memory.****Figure 4: Effect of increasing  $n$  on the number of pseudocores.**

## 5.1 Running Time and Memory Usage

Table 4 shows the running times for RECURS and STREAM for  $n \in \{2^i \mid i \in \{0, \dots, 7\}\}$ . We used a time limit of twelve hours. Our streaming algorithm STREAM performs very well even on data sets with tens of millions of edges, e.g., the *Wikipedia* data set. STREAM is faster than RECURS for all datasets and all  $n$ . In most cases, the speed-up is significant and up to several orders of magnitude. In general, the running time increases roughly linearly with increasing  $n$ , as expected for both algorithms. Recall that STREAM computes the  $j$ -th order H-index for all  $0 \leq j \leq n$ , where RECURS only computes the value for  $j = n$ . Hence, computing the remaining values for  $0 \leq j \leq n-1$  for RECURS would require additional running time. As expected, the speed-up of STREAM compared to RECURS is higher for the data sets with a high average degree because the asymptotic running time of RECURS contains the node degree as a quadratic factor (see Theorem 5), whereas for STREAM it has the node degree as a linear factor (see Theorem 4). RECURS cannot finish the computations for the *Wikipedia* data set and  $n \geq 64$  within the time limit. STREAM has competitive running times compared to other state-of-the-art temporal centrality measures and core-decompositions—a further

discussion can be found in Section 5.2. The memory usage of both algorithms asymptotically behaves similarly. Figure 3 compares the memory usage for *Hospital* and *Email*. RECURS needs slightly more memory because the multisets  $L$  are maintained on the stack for recursive calls.

## 5.2 Additional Efficiency Comparisons

We additionally compare the running times of our new approach to related centrality measures and core decompositions. We provide the running times of the following methods:

- H-INDEX is the static H-index and  $k$ -CORE is the static  $k$ -core. Both were implemented in C++.
- TC, TWC, TKATZ, and TPR are the temporal closeness, walk, Katz, and PageRank centrality. We used the C++ implementations provided by [53].
- TB is the temporal betweenness centrality using strict temporal path (i.e., temporal paths that are strictly advancing in time for each edge) from [6]. The C++ implementation was provided by the authors.
- $(k, h)$ -CORE with  $h \in \{2, 4, 8\}$  is the  $(k, h)$ -core described in [76]. We used the C++ implementations provided by [53].
- SPAN-CORE is temporal core decomposition from [15]. We used the Cython implementation computing the maximum span-cores provided by the authors.

See Table 7 in the appendix for an overview of the time and space complexities of the centrality measures and core decompositions showing that our  $n$ -temporal H-index has competitive complexities. Which is also verified by the following empirical evaluation. Table 5 shows the running times in seconds. We see that our streaming algorithm for the temporal H-index is for low  $n$ , often significantly faster than the algorithms for the computation of the more demanding temporal closeness and betweenness centrality measures. For  $n = 1$ , STREAM has similar running times as computing the static H-index in the underlying aggregated graph, where the temporal variant is slightly faster in almost all cases. Our algorithm needs more time than the temporal Katz and PageRank computations, which is expected as the former are computable in linear time (see Table 7 in the appendix). In the case of the core decompositions, our streaming algorithm STREAM has higher running times compared to the static  $k$  core and the  $(k, h)$ -cores. The reason is that the latter can be computed in linear time. The implementation of the span cores cannot finish the computations for most data sets due to out-of-memory errors. The reason is that the algorithm needs memory in length of the time interval spanned by the temporal graph.

## 5.3 Effect of the Parameter $n$

Figure 4 shows the effect of increasing  $n \in \{2^i \mid i \in \{0, \dots, 10\}\}$  on the number of out-pseudocores, i.e., distinct node values for the outward  $n$ -th order temporal H-index. Figure 4a shows the results for the data sets with less than 150 pseudocores for  $n = 1$ , and Figure 4b shows the results for the remaining data sets. In both cases, we see how the numbers of pseudocores approach one, i.e., the  $n$ -th order temporal H-index is zero for all nodes, as expected due to Theorem 2. For the data sets with the three highest numbers of average degree, i.e., *Hospital*, *Malawi*, and *Highschool*, the number of pseudocores decreases slower than for the other

**Table 4: Running times in seconds (s). OOT: out of time (time limit 12h).**

Data set	$n = 1$		$n = 2$		$n = 4$		$n = 8$		$n = 16$		$n = 32$		$n = 64$		$n = 128$	
	RECURS	STREAM	RECURS	STREAM	RECURS	STREAM	RECURS	STREAM	RECURS	STREAM	RECURS	STREAM	RECURS	STREAM	RECURS	STREAM
Hospital	0.17	0.00	5.42	0.09	15.97	0.25	37.06	0.57	78.40	1.25	162.55	2.68	328.65	5.92	659.53	14.79
Malawi	1.08	0.00	37.59	0.44	110.09	1.37	255.22	3.43	545.44	7.96	1125.34	18.83	2272.54	42.75	4544.73	107.89
Workplace	0.02	0.00	0.31	0.01	0.88	0.02	2.03	0.04	4.31	0.10	8.83	0.20	17.97	0.46	37.45	0.94
HTMLConf	0.06	0.00	1.12	0.02	3.26	0.06	7.56	0.14	16.17	0.31	33.43	0.67	67.60	1.45	135.38	3.25
Highschool	0.97	0.01	28.84	0.52	85.15	1.46	197.26	3.51	420.99	8.49	864.52	20.58	1747.02	46.36	3506.29	100.60
Email	0.04	0.00	0.74	0.02	2.10	0.04	4.79	0.09	10.27	0.19	21.74	0.39	45.99	0.84	109.81	1.86
FacebookMsg	0.05	0.00	0.43	0.02	1.14	0.04	2.56	0.08	5.52	0.15	11.94	0.31	26.70	0.64	63.89	1.48
Infectious	0.53	0.05	3.07	0.19	8.35	0.46	18.81	1.02	39.87	1.98	76.73	4.19	144.48	8.51	270.94	17.48
FacebookWall	0.92	0.19	4.99	0.67	13.18	1.52	31.11	3.48	69.01	6.03	135.03	11.31	310.44	22.49	575.94	43.46
Enron	2.35	0.08	62.63	0.81	184.38	2.07	411.59	4.89	866.53	11.03	1882.11	24.45	4226.25	52.33	9579.23	122.79
AskUbuntu	0.10	0.04	0.35	0.07	0.69	0.12	1.23	0.21	2.50	0.38	5.31	0.72	13.15	1.44	20.43	3.09
Digg	1.19	0.22	9.71	0.71	26.49	1.61	62.80	3.33	120.30	6.84	229.93	13.83	364.88	27.61	467.20	54.81
Wikipedia	67.36	7.86	855.44	26.85	2207.03	61.29	4863.44	117.03	10332.81	230.70	21998.44	457.65	OOT	861.95	OOT	1794.60
Dblp	10.78	6.64	34.39	19.58	78.12	35.92	168.25	68.18	349.69	124.74	708.33	227.67	867.77	419.43	887.72	827.37
Plickr	19.90	7.27	154.39	32.61	397.31	82.62	870.88	168.92	1767.10	332.29	3323.15	640.81	5373.19	1282.34	6310.73	2626.10
Youtube	14.09	5.38	82.18	48.30	204.97	135.38	454.32	323.65	973.77	739.84	2108.57	1657.65	4519.12	3548.93	7340.79	7316.00

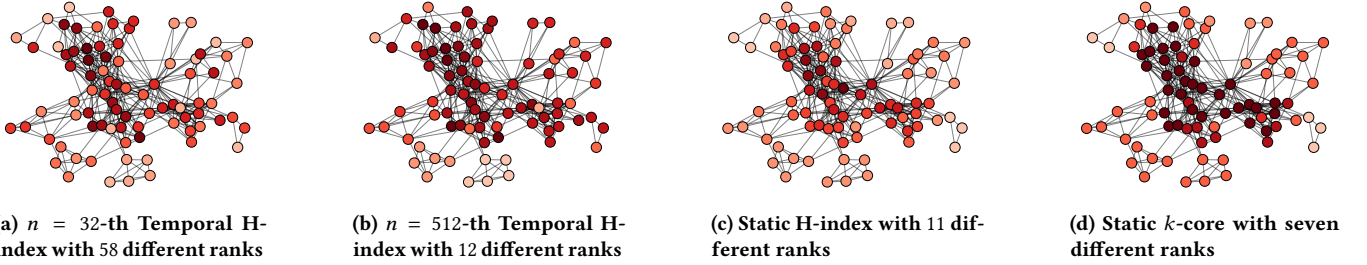


**Figure 5: Comparison of the outward  $n$ -th temporal H-index, the static H-index, and the static  $k$ -core values where a darker color means a higher ranking. The shown network is based on human face-to-face contacts in a village in Malawi.**

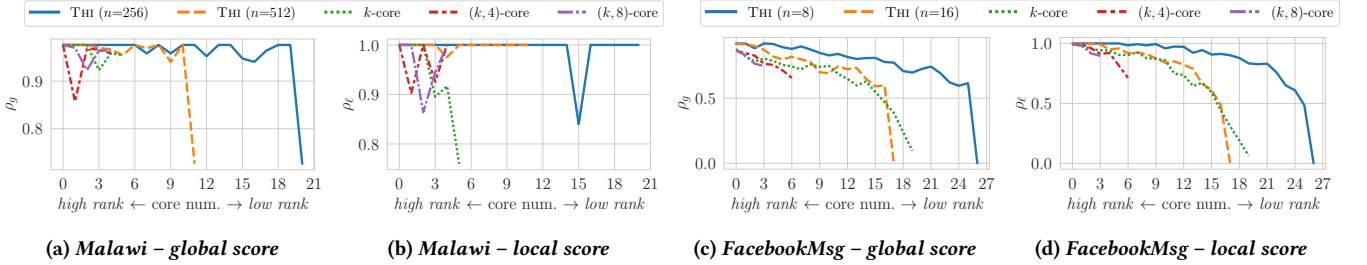


**Figure 6: Comparison of global and local reachability scores of different network decompositions.**

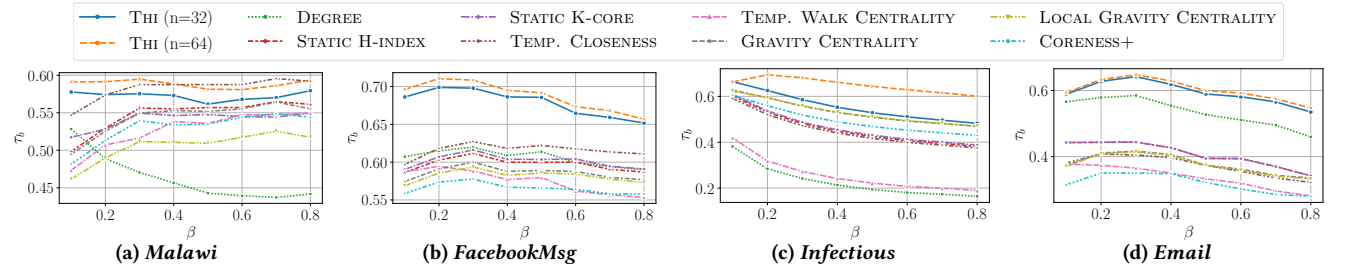


**Figure 7: Kendall  $\tau_b$  correlations between the rankings of different centrality measures and the ranking according to the SIR model for infection probabilities  $\beta \in \{0.1, 0.2, \dots, 0.8\}$ . THI denotes the  $n$ -th order temporal H-index.**

data sets. The reason is that these data sets allow high numbers of temporal walks. In the case of the *Malawi* data set, we see a slight increase in the number of pseudocores from 82 for  $n = 1$  to 83 for  $n = 2$ . This does not conflict with Theorem 2 because even though for individual nodes, the  $n$ -th order temporal H-index approaches

zero for increasing  $n$ , the number of different values of the  $n$ -th order temporal H-index for the nodes can increase.

Algorithm 1 efficiently computes the  $i$ -th order temporal H-index for all  $0 \leq i \leq n$  in one pass. The result allows choosing a decomposition with a number of cores best suited for a downstream task or application. Note that we obtain all non-trivial index values

**Table 5: Running times of related centrality measures and core decompositions in seconds (s). OOT: Out of time (time limit 12h). OOM: Out of memory (available memory 196GB).**

Data set	Centrality Measures						Core Decompositions				
	H-INDEX	Tc	Tb	Twc	Tkatz	Tpr	$k$ -CORE	$(k, 2)$ -CORE	$(k, 4)$ -CORE	$(k, 8)$ -CORE	SPAN-CORE
<i>Hospital</i>	0.00	0.03	90.96	1.89	0.00	0.00	0.00	0.00	0.00	0.00	0.67
<i>Malawi</i>	0.00	0.04	904.13	21.85	0.00	0.00	0.01	0.01	0.01	0.01	2.42
<i>Workplace</i>	0.00	0.03	8.28	0.15	0.00	0.00	0.00	0.00	0.00	0.00	1.38
<i>HTMLConf</i>	0.00	0.05	34.32	0.42	0.00	0.00	0.00	0.00	0.00	0.00	0.37
<i>Highschool</i>	0.00	0.27	2349.55	19.52	0.00	0.01	0.03	0.03	0.03	0.03	1.30
<i>Email</i>	0.00	0.08	109.06	0.23	0.00	0.00	0.01	0.01	0.01	0.01	OOM
<i>FacebookMsg</i>	0.00	0.23	212.94	0.20	0.00	0.00	0.02	0.02	0.02	0.02	OOM
<i>Infectious</i>	0.01	0.90	988.09	1.23	0.00	0.01	0.07	0.07	0.07	0.07	OOM
<i>FacebookWall</i>	0.48	257.02	OOM	3.42	0.01	0.03	1.62	1.08	1.08	1.08	OOM
<i>Enron</i>	0.05	63.20	OOM	10.78	0.01	0.02	0.69	0.59	0.56	0.54	OOM
<i>AskUbuntu</i>	0.05	32.56	OOM	0.23	0.01	0.00	0.37	0.20	0.20	0.20	OOM
<i>Digg</i>	0.51	608.37	OOM	1.74	0.00	0.04	3.86	2.45	2.17	2.17	OOM
<i>Wikipedia</i>	18.46	OOT	OOM	152.32	0.47	1.17	182.75	110.48	94.44	94.33	OOM
<i>Dblp</i>	7.82	OOT	OOM	19.16	0.18	0.39	24.86	14.07	11.88	11.52	OOM
<i>Flickr</i>	11.77	OOT	OOM	60.24	0.28	0.85	80.93	41.57	33.35	34.34	OOM
<i>Youtube</i>	7.83	OOT	OOM	26.13	0.29	0.59	31.39	12.97	13.02	13.14	OOM

for  $0 \leq n \leq \Delta(\mathcal{G})$  and that  $\Delta(\mathcal{G})$ , i.e., the maximal length of a temporal walk, is at most the number of availability times in  $\mathcal{G}$ .

#### 5.4 Temporal Characteristics and Use Case

We first discuss the temporal characteristics of the  $n$ -th order temporal H-index. Due to the space restrictions, we focus on the outward variant. See Appendix C.2 for a comparison of node rankings computed with the inward and outward  $n$ -th order temporal H-indices.

Figure 5 shows an example of the outward  $n$ -th order temporal H-index applied to the *Malawi* network, which is a human face-to-face contact network [55]. Figures 5a to 5d show the aggregated underlying static graph, and the nodes are colored according to their centrality/core value. Figures 5a and 5b show the results for the outward  $n$ -th order temporal H-index, and  $n = 32$  and  $n = 512$ , respectively. The values and range of values are higher for  $n = 32$  compared to  $n = 512$ , as expected due to Theorem 2. Figures 5c and 5d show the values of the static H-index and  $k$ -core numbers of the aggregated graph  $A(\mathcal{G})$  for comparison. First, we note that the  $n$ -th order temporal H-index differentiates more nodes than the static H-index and  $k$ -cores. Respecting the temporal reachability constraints leads to different node rankings compared to the static versions, and the nodes are assigned different (relative) importance.

More specifically, using the outward  $n$ -th temporal H-index, nodes with a strong ability to reach other nodes are ranked high. To verify this property, we measure the *local and global reachability* of out-pseudocores. Let  $\mathcal{G} = (V, \mathcal{E})$  be a temporal graph, and  $r: V \times V \rightarrow \{0, 1\}$  the indicator function for temporal reachability, i.e.,  $r(u, v) = 1$  iff  $u$  can reach  $v$  via a temporal walk. We define the global and local *reachability scores*  $\rho_g$  and  $\rho_\ell$  of a pseudocore  $\mathcal{G}_{(n,k)} = (V', \mathcal{E}')$  as

$$\rho_g = \frac{\sum_{u \in V', v \in V} r(u, v)}{|V'| \cdot |V|}, \text{ and } \rho_\ell = \frac{\sum_{u, v \in V'} r(u, v)}{|V'|^2}, \text{ respectively.}$$

Figure 6 shows the global and local reachability scores for the *Malawi* contact network and the *FacebookMsg* communication network. We show the scores for the  $n$ -th temporal H-index and the static  $k$ -core. We choose two values for  $n$ , where the first equals  $2^i$  where  $i$  is chosen such that there are at least 20 different ranks, i.e.,

$n = 256$  for *Malawi* and  $n = 8$  for *FacebookMsg*, and additionally, we choose  $2^{i+1}$ . Furthermore, as an additional baseline, we use the temporal  $(k, h)$ -core from [76] where we choose  $h \in \{4, 8\}$ . In a  $(k, h)$ -core, each node has at least  $k$  neighbors and at least  $h$  temporal edges to each neighbor. The  $x$ -axes in Figure 6 show cores by ordered rank from zero to the number of cores minus one, where  $x = 0$  corresponds to the highest-ranked core. The results verify that our outward  $n$ -th order temporal H-index leads to pseudocores characterized by high local and global temporal reachability. We discuss the sizes of the cores in Appendix C.3. The nodes in a high-ranked pseudocore, i.e., with a high  $n$ -th order H-index, can, on average, reach many of the nodes of the graph (global), and the nodes in the pseudocore (local). We verify the usefulness of this important property with the following use case.

**5.4.1 Use Case: Influential Spreader Identification.** We evaluate how well the outward  $n$ -th order temporal H-index captures the node influences of spreading processes. Here, we use the stochastic *susceptible-infected-recovered* (SIR) spreading model in temporal networks, which is commonly applied to analyze information or disease dissemination [23, 59, 77]. We give a detailed description in Appendix C.4. We follow the standard practice of recent works, e.g., [37–39, 42], to compare the rankings obtained by centrality measures with the ranking obtained by applying the SIR model. We chose two face-to-face (*Malawi* and *Infectious*) and two communication networks (*FacebookMsg* and *Email*) for the experiment. We chose different infection probabilities  $\beta$  and computed for each  $\beta$  and node  $u \in V$  the mean node influence  $R_u$  over 1000 independent SIR simulations leading to the SIR node rankings. We then compare the SIR rankings with those obtained by the centrality measures using the Kendall  $\tau_b$  rank correlation measure (Appendix C.1). As baselines, we use the static variants of the *degree centrality*, *H-index*, and *k-core*, which are common and popular heuristics for identifying strong spreaders [39]. Furthermore, we used the *temporal closeness centrality*, which was suggested as a strong heuristic for the case of temporal networks in [51, 52], and the recently proposed *temporal walk centrality* [54]. Finally, we use the state-of-the-art

heuristics (*local gravity centrality* [35, 40] and extended neighborhood coreness (*coreness+*) [2], which belong to the best performing  $k$ -core based heuristics as shown in a recent survey [42]. For the  $n$ -th order temporal H-index (THI), we set  $n = 32$  and  $n = 64$ , to include a sufficient neighborhood sizes and to consider sufficient depths of the computation. Figure 7 shows the results. Node rankings obtained from the  $n$ -th order temporal H-index have, in almost all cases, a higher mean correlation to the SIR ranking than the node rankings from the baselines. Only for the *Malawi* data set, the temporal closeness achieves higher correlations. In conclusion, the temporal H-index often indicates the nodes' capabilities for spreading disease or information better than the baselines.

## 6 CONCLUSION

We generalized the static  $n$ -th order H-index for temporal networks. We obtained meaningful variants by taking into account the restricted reachability caused by temporal dynamics. Our streaming algorithm for the common case of uniform transition times is highly scalable. In our experiments, we demonstrated the efficiency and effectiveness of our new approaches. Finally, we showed that the  $n$ -th order temporal H-index could successfully identify super-spreaders in a use-case. In future work, we plan to utilize the pseudocore decomposition to detect cohesive temporal communities and visualize temporal networks.

## ACKNOWLEDGEMENTS

This work is funded by the Deutsche Forschungsgemeinschaft (DFG, German Research Foundation) under Germany's Excellence Strategy–EXC-2047/1–390685813. This research has been funded by the Federal Ministry of Education and Research of Germany and the state of North-Rhine Westphalia as part of the Lamarr-Institute for Machine Learning and Artificial Intelligence, LAMARR22B. This research is supported by the ERC Advanced Grant REBOUND (834862) and the EC H2020 RIA project SoBigData++ (871042). Nils Kriege was supported by the Vienna Science and Technology Fund (WWTF) [10.47379/VRG19009].

## REFERENCES

- [1] J Ignacio Alvarez-Hamelin, Luca Dall'Asta, Alain Barrat, and Alessandro Vespignani. 2006. How the  $k$ -core decomposition helps in understanding the internet topology. In *ISMA Workshop on the Internet Topology*, Vol. 1.
- [2] Joonhyun Bae and Sangwook Kim. 2014. Identifying and ranking influential spreaders in complex networks by neighborhood coreness. *Physica A: Statistical Mechanics and its Applications* 395 (2014), 549–559.
- [3] Vladimir Batagelj and Matjaz Zaversnik. 2003. An  $O(m)$  algorithm for cores decomposition of networks. *arXiv preprint cs/0310049* (2003).
- [4] Ferenc Béres, Róbert Pálovics, Anna Oláh, and András A. Benczúr. 2018. Temporal walk based centrality metric for graph streams. *Applied Network Science* 3, 1 (2018), 32:1–32:26. <https://doi.org/10.1007/s41109-018-0080-5>
- [5] Ulrik Brandes. 2001. A faster algorithm for betweenness centrality. *The Journal of Mathematical Sociology* 25, 2 (2001), 163–177.
- [6] Sebastian Buß, Hendrik Molter, Rolf Niedermeier, and Maciej Rymar. 2020. Algorithmic Aspects of Temporal Betweenness. In *KDD '20: The 26th ACM SIGKDD Conference on Knowledge Discovery and Data Mining*, Rajesh Gupta, Yan Liu, Jiliang Tang, and B. Aditya Prakash (Eds.). ACM, 2084–2092. <https://doi.org/10.1145/3394486.3403259>
- [7] Julián Candia, Marta C González, Pu Wang, Timothy Schoenharl, Greg Madey, and Albert-László Barabási. 2008. Uncovering individual and collective human dynamics from mobile phone records. *Journal of physics A: mathematical and theoretical* 41, 22 (2008), 224015.
- [8] Augustin Chaintreau, Abderrahmen Mtibaa, Laurent Massoulié, and Christophe Diot. 2007. The diameter of opportunistic mobile networks. In *Proceedings of the 2007 ACM Conference on Emerging Network Experiment and Technology*, CoNEXT, Jim Kurose and Henning Schulzrinne (Eds.). ACM, 12. <https://doi.org/10.1145/1364654.1364670>
- [9] Martino Ciaperoni, Edoardo Galimberti, Francesco Bonchi, Ciro Cattuto, Francesco Gullo, and Alain Barrat. 2020. Relevance of temporal cores for epidemic spread in temporal networks. *Scientific reports* 10, 1 (2020), 1–15.
- [10] Pierluigi Crescenzi, Clémence Magnien, and Andrea Marino. 2020. Finding Top- $k$  Nodes for Temporal Closeness in Large Temporal Graphs. *Algorithms* 13, 9 (2020), 211.
- [11] Kousik Das, Sovan Samanta, and Madhumangal Pal. 2018. Study on centrality measures in social networks: a survey. *Soc. Net. Ana. and Min.* 8, 1 (2018), 13.
- [12] Jean-Pierre Eckmann, Elisha Moses, and Danilo Sergi. 2004. Entropy of dialogues creates coherent structures in e-mail traffic. *Proceedings of the National Academy of Sciences* 101, 40 (2004), 14333–14337.
- [13] Şirag Erkol, Dario Mazzilli, and Filippo Radicchi. 2020. Influence maximization on temporal networks. *Physical Review E* 102, 4 (2020), 042307.
- [14] Şirag Erkol, Dario Mazzilli, and Filippo Radicchi. 2022. Effective submodularity of influence maximization on temporal networks. *Physical Review E* 106, 3 (2022), 034301.
- [15] Edoardo Galimberti, Martino Ciaperoni, Alain Barrat, Francesco Bonchi, Ciro Cattuto, and Francesco Gullo. 2020. Span-core decomposition for temporal networks: Algorithms and applications. *ACM TKDD* 15, 1 (2020), 1–44.
- [16] Liang Gao, Senbin Yu, Menghui Li, Zhesi Shen, and Ziyu Gao. 2019. Weighted h-index for Identifying Influential Spreaders. *Symmetry* 11, 10 (2019), 1263.
- [17] Mathieu Génois and Alain Barrat. 2018. Can co-location be used as a proxy for face-to-face contacts? *EPJ Data Science* 7, 1 (2018), 11.
- [18] Felipe Grando, Diego Noble, and Luis C Lamb. 2016. An analysis of centrality measures for complex and social networks. In *2016 IEEE Global Communications Conference (GLOBECOM)*. IEEE, 1–6.
- [19] Peter Grindrod, Mark C. Parsons, Desmond J Higham, and Ernesto Estrada. 2011. Communicability across evolving networks. *Physical Review E* 83, 4 (2011), 046120.
- [20] Jorge E Hirsch. 2005. An index to quantify an individual's scientific research output. *Proceedings of the National Academy of Sciences* 102, 46 (2005), 16569–16572.
- [21] Tad Hogg and Kristina Lerman. 2012. Social dynamics of digg. *EPJ Data Science* 1, 1 (2012), 5.
- [22] Petter Holme. 2015. Modern temporal network theory: A colloquium. *The European Physical Journal B* 88, 9 (2015), 234.
- [23] Petter Holme. 2021. Fast and principled simulations of the SIR model on temporal networks. *Plos one* 16, 2 (2021), e0246961.
- [24] Petter Holme, Christofer R Edling, and Fredrik Liljeros. 2004. Structure and time evolution of an Internet dating community. *Social Networks* 26, 2 (2004), 155–174.
- [25] Wei-Chun Hung and Chih-Ying Tseng. 2021. Maximum (L, K)-Lasting Cores in Temporal Social Networks. In *International Conference on Database Systems for Advanced Applications*. Springer, 336–352.
- [26] Lorenza Isella, Juliette Stehlé, Alain Barrat, Ciro Cattuto, Jean-François Pinton, and Wouter Van den Broeck. 2011. What's in a crowd? Analysis of face-to-face behavioral networks. *Journal of Theor. Biol.* 271, 1 (2011), 166–180.
- [27] Leo Katz. 1953. A new status index derived from sociometric analysis. *Psychometrika* 18, 1 (1953), 39–43.
- [28] Maurice G. Kendall. 1938. A new measure of rank correlation. *Biometrika* 30, 1/2 (1938), 81–93.
- [29] Hyounghick Kim and Ross Anderson. 2012. Temporal node centrality in complex networks. *Physical Review E* 85, 2 (2012), 026107.
- [30] Bryan Klimt and Yiming Yang. 2004. The enron corpus: A new dataset for email classification research. In *European Conference on Machine Learning*. Springer, 217–226.
- [31] Yi-Xiu Kong, Gui-Yuan Shi, Rui-Jie Wu, and Yi-Cheng Zhang. 2019.  $k$ -core: Theories and applications. *Physics Reports* 832 (2019), 1–32.
- [32] Andrea Landherr, Bettina Friedl, and Julia Heidemann. 2010. A critical review of centrality measures in social networks. *Business & Information Systems Engineering* 2, 6 (2010), 371–385.
- [33] Matthieu Latapy, Tiphaine Viard, and Clémence Magnien. 2018. Stream graphs and link streams for the modeling of interactions over time. *Soc. Netw. Anal. Min.* 8, 1 (2018), 61:1–61:29.
- [34] Michael Ley. 2002. The DBLP Computer Science Bibliography: Evolution, Research Issues, Perspectives. In *Proc. Int. Sym. on Str. Proc. and Inf. Retr.* 1–10.
- [35] Hanwen Li, Qiuyan Shang, and Yong Deng. 2021. A generalized gravity model for influential spreaders identification in complex networks. *Chaos, Solitons & Fractals* 143 (2021), 110456.
- [36] Rong-Hua Li, Jiao Su, Lu Qin, Jeffrey Xu Yu, and Qiangqiang Dai. 2018. Persistent community search in temporal networks. In *2018 IEEE 34th International Conference on Data Engineering (ICDE)*. IEEE, 797–808.
- [37] Zhe Li, Tao Ren, Xiaoli Ma, Simiao Liu, Yixin Zhang, and Tao Zhou. 2019. Identifying influential spreaders by gravity model. *Scientific reports* 9, 1 (2019), 1–7.
- [38] Qiang Liu, Yu-Xiao Zhu, Yan Jia, Lu Deng, Bin Zhou, Jun-Xing Zhu, and Peng Zou. 2018. Leveraging local h-index to identify and rank influential spreaders in networks. *Physica A: Statistical Mechanics and its Applications* 512 (2018),

- 379–391.
- [39] Linyuan Lü, Tao Zhou, Qian-Ming Zhang, and H Eugene Stanley. 2016. The H-index of a network node and its relation to degree and coreness. *Nature communications* 7, 1 (2016), 1–7.
- [40] Ling-ling Ma, Chuang Ma, Hai-Feng Zhang, and Bing-Hong Wang. 2016. Identifying influential spreaders in complex networks based on gravity formula. *Physica A: Statistical Mechanics and its Applications* 451 (2016), 205–212.
- [41] Clémence Magnien and Fabien Tarissan. 2015. Time evolution of the importance of nodes in dynamic networks. In *ASONAM*. IEEE, 1200–1207.
- [42] Giridhar Maji, Sharmistha Mandal, and Soumya Sen. 2020. A systematic survey on influential spreaders identification in complex networks with a focus on K-shell based techniques. *Expert Syst. with App.* 161 (2020), 113681.
- [43] Fragkiskos D Malliaros, Christos Giatsidis, Apostolos N Papadopoulos, and Michalis Vazirgiannis. 2020. The core decomposition of networks: Theory, algorithms and applications. *The VLDB Journal* 29, 1 (2020), 61–92.
- [44] Rossana Mastrandrea, Julie Fournet, and Alain Barrat. 2015. Contact patterns in a high school: a comparison between data collected using wearable sensors, contact diaries and friendship surveys. *PLoS one* 10, 9 (2015), e0136497.
- [45] Othon Michail. 2016. An Introduction to Temporal Graphs: An Algorithmic Perspective. *Internet Math.* 12, 4 (2016), 239–280. <https://doi.org/10.1080/15427951.2016.1177801>
- [46] Alan Mislove, Hema Swetha Koppula, Krishna P Gummadi, Peter Druschel, and Bobby Bhattacharjee. 2008. Growth of the flickr social network. In *Proceedings of the first workshop on Online social networks*. 25–30.
- [47] Alan Mislove, Massimiliano Marcon, P. Krishna Gummadi, Peter Druschel, and Bobby Bhattacharjee. 2007. Measurement and analysis of online social networks. In *Proceedings of the 7th ACM SIGCOMM Internet Measurement Conference, IMC*. ACM, 29–42.
- [48] Alan E. Mislove. 2009. *Online social networks: measurement, analysis, and applications to distributed information systems*. Ph.D. Dissertation. Rice University.
- [49] Petra Mutzel and Lutz Oettershagen. 2019. On the enumeration of bicriteria temporal paths. In *TAMC*. Springer, 518–535.
- [50] Vincenzo Nicosia, John Tang, Cecilia Mascolo, Mirco Musolesi, Giovanni Russo, and Vito Latora. 2013. Graph metrics for temporal networks. In *Temporal Networks*. Springer, 15–40.
- [51] Lutz Oettershagen and Petra Mutzel. 2020. Efficient top-k temporal closeness calculation in temporal networks. In *2020 IEEE International Conference on Data Mining (ICDM)*. IEEE, 402–411.
- [52] Lutz Oettershagen and Petra Mutzel. 2022. Computing top-k temporal closeness in temporal networks. *KAIS* (2022), 1–29.
- [53] Lutz Oettershagen and Petra Mutzel. 2022. Tglib: an open-source library for temporal graph analysis. *arXiv preprint arXiv:2209.12587* (2022).
- [54] Lutz Oettershagen, Petra Mutzel, and Nils M Kriege. 2022. Temporal Walk Centrality: Ranking Nodes in Evolving Networks. In *Proceedings of the ACM Web Conference 2022*. 1640–1650.
- [55] Laura Ozella, Daniela Paolotti, Guilherme Lichand, Jorge P Rodríguez, Simon Haenni, John Phuka, Onicio B Leal-Neto, and Ciro Cattuto. 2021. Using wearable proximity sensors to characterize social contact patterns in a village of rural Malawi. *EPJ Data Science* 10, 1 (2021), 46.
- [56] Raj Kumar Pan and Jari Saramäki. 2011. Path lengths, correlations, and centrality in temporal networks. *Physical Review E* 84, 1 (2011), 016105.
- [57] Pietro Panzarasa, Tore Opsahl, and Kathleen M. Carley. 2009. Patterns and dynamics of users' behavior and interaction: Network analysis of an online community. *Journal of the American Society for Information Science and Technology* 60, 5 (2009), 911–932.
- [58] Ashwin Paranjape, Austin R. Benson, and Jure Leskovec. 2017. Motifs in temporal networks. In *Proceedings of the Tenth ACM International Conference on Web Search and Data Mining*. 601–610.
- [59] Sen Pei, Lev Muchnik, Shaoting Tang, Zhiming Zheng, and Hernán A Makse. 2015. Exploring the complex pattern of information spreading in online blog communities. *PLoS one* 10, 5 (2015), e0126894.
- [60] Hongchao Qin, Rong-Hua Li, Guoren Wang, Xin Huang, Ye Yuan, and Jeffrey Xu Yu. 2020. Mining Stable Communities in Temporal Networks by Density-based Clustering. *IEEE Transactions on Big Data* (2020).
- [61] Hongchao Qin, Rong-Hua Li, Guoren Wang, Lu Qin, Ye Yuan, and Zhiwei Zhang. 2019. Mining bursting communities in temporal graphs. *arXiv preprint arXiv:1911.02780* (2019).
- [62] Francisco Aparecido Rodrigues. 2019. Network centrality: an introduction. In *A Mathematical Modeling Approach from Nonlinear Dynamics to Complex Systems*. Springer, 177–196.
- [63] Giulio Rossetti and Rémy Cazabet. 2018. Community discovery in dynamic networks: a survey. *ACM computing surveys (CSUR)* 51, 2 (2018), 1–37.
- [64] Ryan A. Rossi and Nesreen K. Ahmed. 2015. The Network Data Repository with Interactive Graph Analytics and Visualization. In *AAAI*. <https://networkrepository.com>
- [65] Polina Rozenshtein and Aristides Gionis. 2016. Temporal PageRank. In *Machine Learning and Knowledge Discovery in Databases - European Conference, ECML PKDD (Lecture Notes in Computer Science, Vol. 9852)*. Springer, 674–689.
- [66] Diego Santoro and Ilie Sarpe. 2022. ONBRA: Rigorous Estimation of the Temporal Betweenness Centrality in Temporal Networks. In *Proceedings of the ACM Web Conference 2022*. 1579–1588.
- [67] Nicola Santoro, Walter Quattrociochi, Paola Flocchini, Arnaud Casteigts, and Frederic Amblard. 2011. Time-varying graphs and social network analysis: Temporal indicators and metrics. *arXiv preprint arXiv:1102.0629* (2011).
- [68] Akрати Saxena and Sudarshan Iyengar. 2020. Centrality Measures in Complex Networks: A Survey. *CoRR abs/2011.07190* (2020). [arXiv:2011.07190](https://arxiv.org/abs/2011.07190) <https://arxiv.org/abs/2011.07190>
- [69] Kijung Shin, Tina Eliassi-Rad, and Christos Faloutsos. 2016. Corescope: Graph mining using k-core analysis—patterns, anomalies and algorithms. In *2016 IEEE 16th international conference on data mining (ICDM)*. IEEE, 469–478.
- [70] John Tang, Ilias Leontiadis, Salvatore Scellato, Vincenzo Nicosia, Cecilia Mascolo, Mirco Musolesi, and Vito Latora. 2013. Applications of temporal graph metrics to real-world networks. In *Temporal Networks*. Springer, 135–159.
- [71] John Tang, Mirco Musolesi, Cecilia Mascolo, Vito Latora, and Vincenzo Nicosia. 2010. Analysing information flows and key mediators through temporal centrality metrics. In *Proc. 3rd Workshop on Social Network Systems*. 1–6.
- [72] Ioanna Tsalouchidou, Ricardo Baeza-Yates, Francesco Bonchi, Kewen Liao, and Timos Sellis. 2019. Temporal betweenness centrality in dynamic graphs. *International Journal of Data Science and Analytics* (2019), 1–16.
- [73] Philippe Vanhems, Alain Barrat, Ciro Cattuto, Jean-François Pinton, Naghm Khanafer, Corinne Régis, Byeul-a Kim, Brigitte Comte, and Nicolas Voirin. 2013. Estimating potential infection transmission routes in hospital wards using wearable proximity sensors. *PLoS one* 8, 9 (2013), e73970.
- [74] Bimal Viswanath, Alan Mislove, Meeyoung Cha, and Krishna P. Gummadi. 2009. On the evolution of user interaction in facebook. In *Proceedings of the 2nd ACM workshop on Online social networks*. 37–42.
- [75] Huanhuan Wu, James Cheng, Silu Huang, Yiping Ke, Yi Lu, and Yanyan Xu. 2014. Path problems in temporal graphs. *Proc. VLDB End.* 7, 9 (2014), 721–732.
- [76] Huanhuan Wu, James Cheng, Yi Lu, Yiping Ke, Yuzhen Huang, Da Yan, and Hejun Wu. 2015. Core decomposition in large temporal graphs. In *2015 IEEE International Conference on Big Data (Big Data)*. IEEE, 649–658.
- [77] Shilun Zhang, Xunyi Zhao, and Huijuan Wang. 2022. Mitigate SIR epidemic spreading via contact blocking in temporal networks. *Applied network science* 7, 1 (2022), 1–22.

## APPENDIX

We provide the omitted proofs and additional results. Table 6 gives an overview of commonly used notations.

### A OMITTED PROOFS

**PROOF OF LEMMA 1.** We use induction over the distances in the induced subtree  $\Gamma_n^*(v) \subseteq \Gamma(v)$  that only contains nodes  $u \in U$  with  $d(u) \leq n + 1$ . Our base case considers nodes  $\ell \in U$  with  $d(\ell) = n$  for which  $\phi_n(\ell) = (w, t) = |\mathcal{C}(\ell)| = \delta^*(w, t) = h_{w,t,\star}^{(n-d(\ell))}$ . Now we consider an inner node  $u = (w, t)$  of the tree and assume the statement holds for all its children  $C(u)$ . Hence,

$$\begin{aligned} \phi_n(u) &= \mathcal{H}(\{\phi_n(c) \mid c \in C(u)\}) = \mathcal{H}(\{h_{w_i,t_i,\star}^{(n-d(w_i))} \mid (w_i, t_i) \in C(u)\}) \\ &= \mathcal{H}(\{h_{w_i,t_i,\star}^{(n-d(u)+1)} \mid (w_i, t_i) \in \mathcal{N}\}) = h_{w,t,\star}^{(n-d(u))} \end{aligned}$$

□

**PROOF OF THEOREM 1.** Due to ?? the root  $r$  has at least  $k$  children  $C(r)$  because  $h_{v,t,\star}^{(0)} \geq k$ . For each  $(w, t) \in C(r)$  of the children, we can argue that  $h_{w,t,\star}^{(1)} \geq k$ . Similar we can argue that in each depth level up to  $n$  of  $\Gamma^*(v)$  each node has at least  $k$  children. Hence, the total number of descendants is at least  $\sum_{i=1}^{n+1} k^i = \frac{k^{n+2} - k}{k-1}$ . □

**PROOF OF THEOREM 2.** Consider the reachability tree  $\Gamma^*(v)$  of the node  $v$ . Let  $d(\Gamma^*(v))$  be the maximal depths of the tree which is upper bounded by  $\Delta(\mathcal{G})$ . Recall that  $\Delta(\mathcal{G})$  is the temporal diameter of  $\mathcal{G}$ , i.e., an upper bound for the maximal number of edges in any walk in  $\mathcal{G}$ . Then, for  $n > d(\Gamma^*)$  it follows that for each leaf  $\ell$  in  $\Gamma^*(v)$ ,  $\phi_n(\ell) = 0$  because  $n > d(\Gamma^*) \geq d(\ell)$ . Moreover, the depths

**Table 6: Commonly used notations**

Symbol	Definition
$G = (V, E)$	finite static graph with set of nodes $V$ and undirected edges $E \subseteq \{\{u, v\} \subseteq V \mid u \neq v\}$
$\mathcal{G} = (V, \mathcal{E})$	finite temporal graph $\mathcal{G}$ with nodes $V$ and temp. edges $\mathcal{E}$
$e = (u, v, t, \lambda)$	temporal $(u, v)$ -edge at time $t$ with transition time $\lambda$
$\Delta(\mathcal{G})$	the length of the longest (in # of edges) temporal walk in $\mathcal{G}$
$\delta_{\max}^-(\mathcal{G}), \delta_{\max}^+(\mathcal{G})$	maximal in-degree and out-degrees of $\mathcal{G}$
$h_{v,-}^{(n)}$	outward $n$ -th order temporal H-index of a node $v \in V$
$h_{v,+}^{(n)}$	inward $n$ -th order temporal H-index of a node $v \in V$
$N^-(u, t)$	time-dependent in-neighborhood of a node $u$ at time $t$ , i.e., $\{(v, u, t_e, \lambda_e) \in \mathcal{E} \mid t_e + \lambda_e \leq t\}$
$N^+(u, t)$	time-dependent out-neighborhood of a node $u$ at time $t$ , i.e., $\{(u, v, t_e, \lambda_e) \in \mathcal{E} \mid t_e \geq t\}$
$\mathcal{N}^-(v, t)$	all pairs of nodes and starting times $(w, t_w)$ such that there exists a temporal edge $(w, v, t_w, \lambda) \in \mathcal{E}$ with $t_w + \lambda \leq t$
$\mathcal{N}^+(v, t)$	multiset of pairs of nodes and times $(w, t_w)$ s.t. there is a temporal edge $(v, w, t', \lambda) \in \mathcal{E}$ with arrival time $t_w = t' + \lambda$ and $t' \geq t$
$\mathcal{H}: S \rightarrow \mathbb{N}_0$	for $S \subseteq \{\{s \mid s \in \mathbb{N}_0\}\}$ the max. $i$ s.t. at least $i$ elements $s \in S$ with $s \geq i$
$\Gamma^-(v), \Gamma^+(v)$	inward and outward reachability trees
$d(u)$	depth of $u \in V(\Gamma^*(v))$ with $\star \in \{-, +\}$

of the ancestors  $\ell$  in  $\Gamma^*(v)$  is strictly smaller than  $d(\ell)$ . Hence, the case that  $n = d(u)$  in Definition 5 cannot be reached and due to Lemma 1 the result follows.  $\square$

**PROOF OF THEOREM 3.** The first containment property,  $\mathcal{G}_{(n,0)} \supseteq \mathcal{G}_{(n,1)} \supseteq \dots \supseteq \mathcal{G}_{(n,\tau_n-1)} \supseteq \mathcal{G}_{(n,\tau_n)}$ , follows directly from Definition 6. To prove the second containment property,  $\mathcal{G}_{(0,k)} \supseteq \mathcal{G}_{(1,k)} \supseteq \dots \supseteq \mathcal{G}_{(\eta_k-1,k)} \supseteq \mathcal{G}_{(\eta_k,k)}$ , let  $\Gamma^*(v) = (U, E, r)$  be a reachability tree of any node  $v \in V$ . We show that  $\phi_n(r) \geq \phi_{n+1}(r)$  which together with Lemma 1 proves the statement. Let  $p \in U$  be a node  $\Gamma^*(v)$  with  $d(p) = n$  and therefore  $\phi_n(p) = |C(p)|$  which is an upper bound on  $\phi_n(p)$  for all  $n \in \mathbb{N}$ . Moreover, we have  $\phi_{n+1}(p) = \mathcal{H}(\{|C(p)| \mid c \in C(p)\})$  with  $C(p)$  being the set of children of  $p$ . And,  $\mathcal{H}(\{|C(p)| \mid c \in C(p)\})$  is also upper bounded by  $|C(p)|$ . Hence,  $\phi_n(p) \geq \phi_{n+1}(p)$ . We now assume the statement holds for all children  $c \in C(u)$  of some node  $u \in U$ . By induction, it follows that  $\phi_n(u) = \mathcal{H}(\{\phi_n(c) \mid c \in C(u)\}) \geq \mathcal{H}(\{\phi_{n+1}(c) \mid c \in C(u)\}) = \phi_{n+1}(u)$ . Hence, the result follows.  $\square$

Before we prove Theorem 4, we introduce the following lemmas.

**Lemma 2.** *Let  $t_\ell$  be the latest time stamp such that Algorithm 1 processed all edges with availability time  $t_\ell$ . At any iteration of the for-loop in line 6, when processing the temporal edge  $e = (u, v, t)$ , it holds  $\deg[u] = \delta^+(u, t_\ell)$  and  $\deg[v] = \delta^+(v, t_\ell)$ .*

**PROOF.** Algorithm 1 uses  $lt[u]$  to store the last time stamp of an edge leaving node  $u$ . If the time stamp  $t$  of the currently processed edge  $e = (u, v, t)$  is earlier than  $lt[u]$ , i.e.,  $lt[u] > t$ , the algorithm updates the values  $lt[u]$  and  $\deg[u]$  by setting  $lt[u] = t$  and  $\deg[u] = \pi[u][0].length$ . This only happens if all edges with availability times later than  $t$  are processed due to the processing of the edges in reverse chronological order. At this point and due to line 13, the length of  $\pi[u][0]$  equals the number of edges leaving  $u$  up to time  $t$  (not including the current edge  $e$ ). Hence,  $\deg[u] = \delta^+(u, t_\ell)$  until the next update. Similarly, the result holds for  $\deg[v]$ .  $\square$

**Lemma 3.** *After each iteration of the for loop in line 6, processing edge  $e = (u, v, t)$ , the lists  $\pi[w][j]$  contain the values  $X = \{\{(t', h_{y,t'}^{(j)})\}\}$  such that  $\mathcal{H}_t(X) = h_{w,t}^{(j)}$  for all  $1 \leq j \leq n$  and all  $w \in V$ .*

**PROOF.** Let  $e_1, \dots, e_m$  be the sequence of temporal edges in reverse chronological order (ties broken arbitrarily). After processing the first edge  $e_1 = (u_1, v_1, t_1)$  the statement holds with the lists  $\pi[w][j]$  empty and  $h_{w,t_1}^{(j)} = 0$  for  $1 \leq j \leq n$  and all  $w \in V$ . Now assume the statement holds after the  $(k-1)$ -th edge, and we consider the  $k$ -th edge. When  $e_k = (u_k, v_k, t_k)$  arrives all edges with time stamps larger than  $t_k$  have been processed. For  $j = 1$ , by our assumption  $\pi[u_k][j]$  contains pairs  $(t_i, d_i)$  for  $t_i \geq t_k$  such that  $v_i$  is a neighbor that has a temporal degree  $\delta^+(v_i, t') = d_i$  for some  $t' \geq t_i$ . Now after adding  $(t_k, \deg[v_k])$ , it follows that  $\mathcal{H}_{t_k}(\pi[u_k][1]) = \mathcal{H}(\{d_i \mid (t', d_i) \in \pi[u_k][j] \wedge t' + \lambda \geq t_k\}) = h_{u_k, t_k}^{(1)}$ . Similarly, for  $1 \leq j \leq n$ , in line 16 and following, the algorithm appends to each list  $\pi[u_k][j+1]$  the pair  $p = (t_k, \mathcal{H}_{t_k}(\pi[v_k][j]))$ . By applying our assumption, we can rewrite  $p = (t_k, h_{v_k, t_k}^{(j)})$ . And,  $\mathcal{H}_{t_k}(\pi[u_k][j+1]) = \mathcal{H}(\{h_{v_k, t_k}^{(j)} \mid (t', h_{v_k, t_k}^{(j)}) \in \pi[v_k][j] \wedge t' + \lambda \geq t_k\}) = h_{u_k, t_k}^{(j+1)}$ .  $\square$

**PROOF OF THEOREM 4.** The algorithm terminates after iterating over the edges and nodes. The correctness follows from Lemmas 2 and 3. Note for the case of  $n = 0$ , we only need to set  $h_v^{(0)}$  to the length of  $\pi[v][0]$  (see line 19) because due to line 13 the list contains one entry for each outgoing edge from  $v$ .

For the running time, initialization is done in  $O(|V| \cdot n)$  and we iterate over the edges once. In each iteration of the for loop in line 6, we have another loop with  $n$  iterations (line 16). During this second loop, we compute  $\mathcal{H}_t(\pi[v][j])$ . The running time of  $\mathcal{H}_t(\pi[v][j])$  is linear in the length of the list  $\pi[v][j]$  which is upper bounded by the out-degree of node  $v$ . Therefore, for the first for loop a running time of  $O(|\mathcal{E}| \cdot n \cdot \delta_{\max})$  follows. The running time of lines 17–20 is similarly in  $O(|V| \cdot n \cdot \delta_{\max})$ .  $\square$

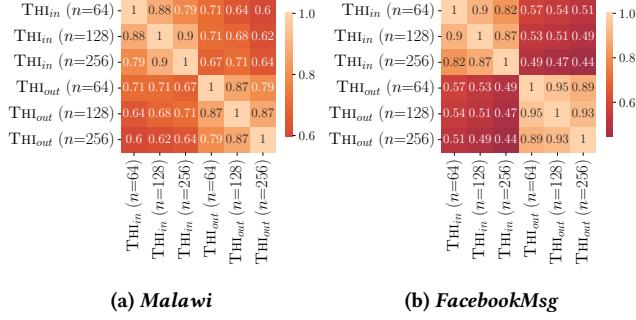


Figure 8: Kendall  $\tau_b$  correlation matrices of the rankings using the inward and outward  $n$ -th order temporal H-index.

## B COMPUTATION

In this section, we describe the naive recursive algorithm and the computation of the inward  $n$ -th order temporal H-index by reversing the temporal graph.

### B.1 Naive Recursive Algorithm

The recursive definition of the temporal  $n$ -th order H-index enables a straightforward top-down approach. We provide the pseudocode in Appendix B. Algorithm 2 shows a recursive algorithm for computing  $h_{v,\star}^{(n)}$  for  $\star \in \{-, +\}$  and all  $v \in V$ , utilizing memoization to avoid recomputation of already computed values of  $h_{v,t,\star}^{(n)}$ .

**THEOREM 5.** Let  $\star \in \{-, +\}$ , Algorithm 2 computes  $h_{v,\star}^{(n)}$  for all  $v \in V$  in time  $O(|V| \cdot n \cdot (\delta_{\max}^{\star})^2)$  with space  $O(|V| \cdot n \cdot \delta_{\max}^{\star})$ .

**PROOF OF THEOREM 5.** The running time and space complexity depend on the total size of  $m[v][i]$  which consists of  $|V| \cdot n$  associative arrays, which can be implemented using perfect hashing as the time steps of the incoming edges at each node are known in advance. Each of the associative arrays contains at most  $\delta_{\max}$  entries, where  $\delta_{\max}$  is the maximum degree in  $\mathcal{G}$ , and the space complexity follows. To obtain each entry of the hash maps, we have to compute  $\mathcal{H}(L)$  in  $O(\delta_{\max})$  time because the size of  $L$  is upper bounded by  $\delta_{\max}$ , leading to the stated running time complexity.

The algorithm terminates due to line 5 and because in each call of the function  $R$  the value of parameter  $n$  is decreased (line 9). We show that  $R(v, n, t) = \phi_n(u = (v, t))$  in the reachability tree  $\Gamma_n(v) = (U, E)$  that contains all nodes  $u \in U$  with depth  $d(u) \leq n+1$ . We use induction over the recursion depths. The maximum depth of the recursion tree is  $n$  due to lines 5 and 9. The base case is for depths  $n$  where we have  $R(v, 0, t) = \delta(v, t) = \phi_n(u = (v, t))$ . Now, for the case of depths  $j < n$ , we consider  $R(v', n-j, t')$  and assume the statement holds for depths larger than  $j$ . Due to lines 8f, and by applying the induction hypothesis it follows that  $L = \{\{R(w, n-1, t+\lambda) \mid (w, w, t, \lambda) \in \mathcal{E}\} = \{\phi_n(c) \mid c \in C(u)\}$ , where  $C(u) \subset U$  is the set of children of the node  $u = (v', t') \in U$  in  $\Gamma_n(v)$ . Therefore,  $R(v', n-j, t') = \mathcal{H}(L) = \phi_n(u = (v', t'))$ . With Lemma 1 the result follows.  $\square$

### Algorithm 2: Algorithm RECURS using memoization

**Input:** Temporal graph  $\mathcal{G} = (V, \mathcal{E})$ ,  $n \in \mathbb{N}$

**Output:**  $h_{v,\star}^{(n)}$  for all  $v \in V$

```

1 Initialize empty array of associative arrays  $m[v][i]$  for all  $v \in V$ 
  and  $i \in [n]$ 
2 Function  $R(v, n, t)$ :
3   if  $m[v][n]$  has entry for  $t$  then
4     return  $m[v][n][t]$ 
5   if  $n = 0$  or  $\delta^{\star}(v, t) = 0$  then
6     return  $\delta^{\star}(v, t)$ 
7   Initialize empty multiset  $L$ 
8   foreach  $e = (v, w, t, \lambda)$  with  $(w, t) \in \mathcal{N}^{\star}(v, t)$  do
9      $L \leftarrow L \cup \{R(w, n-1, t+\lambda)\}$ 
10    (or  $L \leftarrow L \cup \{R(w, n-1, t)\}$  if  $\star = -$ )
11     $m[v][n][t] \leftarrow \mathcal{H}(L)$ 
12  return  $m[v][n][t]$ 
13 Initialize  $h_{v,\star}^{(n)} = 0$  for all  $v \in V$ 
14 foreach  $v \in V$  do
15    $h_{v,\star}^{(n)} = R(v, n, 0)$ 
16 return  $h_{v,\star}^{(n)}$  for all  $v \in V$ 

```

### B.2 Reverse Computation

In order to compute the inward  $n$ -th order temporal H-index using Algorithm 1, we first transform the temporal network  $\mathcal{G}$  using the temporal transpose  $\mathcal{T}(\mathcal{G})$  introduced in [51].

**Definition 8** (Temporal transpose [51]). For a temporal graph  $\mathcal{G} = (V, \mathcal{E})$ , we call  $\mathcal{T}(\mathcal{G}) = (V, \tilde{\mathcal{E}})$  with edge set  $\tilde{\mathcal{E}} = \{(v, u, t_{\max} - t, \lambda) \mid (u, v, t, \lambda) \in \mathcal{E}\}$  and  $t_{\max} = \max\{t + \lambda \mid (u, v, t, \lambda) \in \mathcal{E}\}$  the temporal transpose of  $\mathcal{G}$ .

Computing the temporal transpose is possible in  $O(m)$  time and space. We use the following helpful result.

**PROPOSITION 6.** Let  $\mathcal{G}$  be a temporal graph with equal transition times for all  $e \in \mathcal{E}$  and  $\mathcal{T}(\mathcal{G})$  its temporal transpose. Then,  $h_{v,+}^{(i)}$  in  $\mathcal{T}(\mathcal{G})$  equals  $h_{v,-}^{(i)}$  in  $\mathcal{G}$  for all  $0 \leq i \leq n$  and  $v \in V$ .

**PROOF.** The proposition follows from Lemma 4 in [52].  $\square$

Due to Proposition 6, we can efficiently compute  $h_{v,-}^{(i)}$  for all  $0 \leq i \leq n$  and  $v \in V$  by first computing the temporal transpose  $\mathcal{T}(\mathcal{G})$  and then call Algorithm 1 with  $\mathcal{T}(\mathcal{G})$ .

## C EXPERIMENTAL EVALUATION

We provide additional experimental results and the details.

### C.1 Kendall Rank Correlation

The Kendall rank correlation coefficient is a common and standard way of comparing node rankings and centrality measures [18]. Because node rankings may contain ties, we use the Kendall  $\tau_b$  rank correlation variant that makes adjustments for ties. For the formal definition, please refer to [28]. The Kendall  $\tau_b$  rank correlation takes on values between one and minus one: values close to one indicate

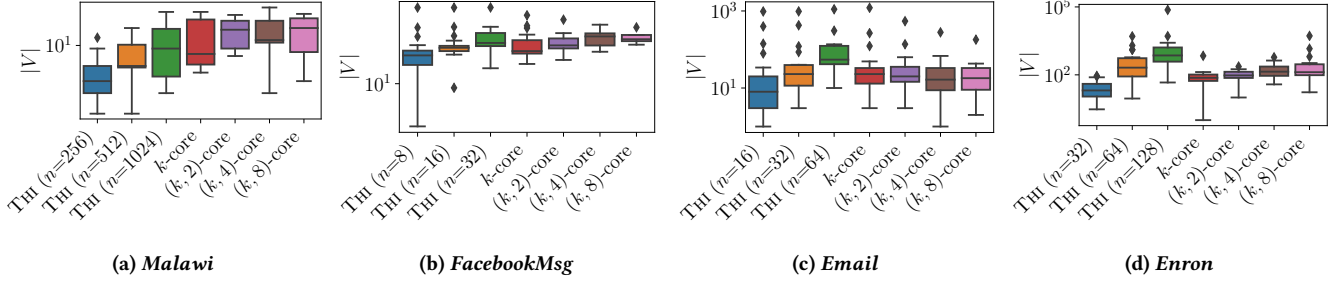


Figure 9: Box-plots of the number of vertices in the computed cores. The  $y$ -axes are logarithmic.

**Table 7: Overview of related centrality measures and core decompositions, with  $\mathcal{T} = \{t \mid (u, v, t, \lambda) \in \mathcal{E}\}$ ,  $\tau_{max}$  the largest cardinality of availability or arrival times at a node,  $T$  the total length of the time interval spanned by the temporal graph, and  $I$  the length of a time window. The time complexities are for computing the centrality or core number all nodes.**

Method	Running Time	Space	Reference
Static H-index	$\mathcal{O}( V  \cdot \delta_{max})$	$\mathcal{O}( V )$	[20]
Temporal Closeness	$\mathcal{O}( V ^2 +  V  \mathcal{E} )$	$\mathcal{O}( V  +  \mathcal{E} )$	[75]
Temporal Betweenness	$\mathcal{O}( V ^3 \cdot \mathcal{T}^2)$	$\mathcal{O}( V  \cdot \mathcal{T} +  \mathcal{E} )$	[6]
Temporal PageRank/Katz	$\mathcal{O}( \mathcal{E} )$	$\mathcal{O}( V )$	[4, 65]
Temporal Walk Centrality	$\mathcal{O}( \mathcal{E}  \cdot \tau_{max})$	$\mathcal{O}( V  \cdot \tau_{max})$	[54]
Static $k$ -Core	$\mathcal{O}( V  +  \mathcal{E} )$	$\mathcal{O}( V )$	[39]
Temporal $(k, h)$ -Core	$\mathcal{O}( V  \cdot \delta_{max})$	$\mathcal{O}( V )$	[76]
Temporal Span-Core	$\mathcal{O}(\mathcal{E} \cdot T^2)$	$\mathcal{O}( \mathcal{E}  + T)$	[15]

similar rankings, close to zero no correlation, and close to minus one a strong negative correlation.

## C.2 Inward vs Outward $n$ -th Temporal H-Index

Figure 8 shows the Kendall  $\tau_b$  correlations between the node rankings obtained by the inward and outward  $n$ -th order temporal H-index for  $n \in \{64, 128, 256\}$ . The correlation between the rankings using inward or outward  $n$ -th order temporal H-index for different  $n$  is high, which we expected. The correlation between rankings obtained from the inward and the outward  $n$ -th order temporal H-index is lower. However, we still observe correlations of at least 0.6 (*Malawi*) and 0.44 (*FacebookMsg*) as there are nodes with high (or low) inward and outward  $n$ -th order temporal H-index in the data sets.

## C.3 Sizes of the Pseudocores

Figure 9 shows boxplots of the vertex set sizes  $|V|$  of the cores for the temporal H-index, the static  $k$  core, and the temporal  $(k, h)$ -cores. We show the results for *Malawi*, *FacebookMsg*, *Email*, and *Enron*. For the temporal H-index, the pseudocore sizes increase with increasing  $n$  because the number of pseudocores decreases (Theorem 2). Hence, the sizes are controllable using the parameter  $n$ .

## C.4 SIR Model

The stochastic *susceptible-infected-recovered* (SIR) spreading model is a standard model for analyzing spreading processes [23, 59]. In

the model, each node is either *susceptible*, *infected*, or *recovered*. We used the SIR model as described in [23] and the implementation for temporal networks provided by the author. In the beginning, a single node  $u \in V$  is infected. The infection can spread along temporal edges with infection probability  $\beta$ . An infected node will recover after time  $\delta$  sampled with probability  $P(\delta) = \nu \exp(-\nu\delta)$  from an exponential distribution, where  $\nu$  is set to 20 time units of the network. At the start of the simulation, a single node is infected. The node influence  $R_u$  of the initially infected node  $u \in V$  is the number of nodes that are either infected or recovered after the simulation finishes, i.e., when no further infections are possible.